

P- 93

Phase A Final Report

**Geostationary Earth Climate Sensor:
Scientific Utility and Feasibility**

by

G.G. Campbell and T.H. Vonder Haar

with contributions by

T. Evert, TRW

Under Contract NAG 8 - 145

*Studies of An Earth Radiation Climate Radiometer (ERCR)
for the Geostationary Earth Observatory (GEO)*

from the

National Aeronautics and Space Administration
Marshall Space Flight Center
Huntsville, Alabama 35812

to the

Cooperative Institute for Research in the Atmosphere
Colorado State University
Fort Collins, Colorado 80523

Co-Principal Investigators:
Thomas H. Vonder Haar
Stanley Q. Kidder

Co-Investigators:
G. Garrett Campbell
James F. W. Purdom

July, 1991

N93-20248

Unclas

0141247

G3/46

(NASA-CR-191919) GEOSTATIONARY
EARTH CLIMATE SENSOR: SCIENTIFIC
UTILITY AND FEASIBILITY, PHASE A
Final Report (Colorado State
Univ.) 93 p

Overview

The possibility of accurate broad band radiation budget measurements from a GEO platform will provide a unique opportunity for viewing radiation processes in the atmosphere-ocean system. The CSU/TRW team has prepared a Phase A instrument design study demonstrating that measurements of radiation budget are practical from geosynchronous orbit with proven technology. This instrument concept is the Geostationary Earth Climate Sensor (GECS). A range of resolutions down to 20 km at the top of the atmosphere are possible, depending upon the scientific goals of the experiment. These tradeoffs of resolution and measurement repeat cycles are examined for scientific utility. The design of a flexible instrument is shown to be possible to meet the two goals: long-term, systematic monitoring of the diurnal cycles of radiation budget; and high time and space resolution studies of regional radiation features.

Subject terms: Earth Radiation Budget
Geosynchronous
Diurnal Measurement System

1. *Introduction*

This report reviews several topics related to the scientific goals of the Geostationary Earth Climate Sensor (GECS). The possibility of geosynchronous radiation budget measurements will improve our understanding of the details of radiative forcing on the Earth atmosphere-ocean system. Measurements of the full diurnal cycle are needed if we are to achieve accuracies needed to monitor climate change. Attached as Appendix I is a report prepared by T. Evert of TRW of a Phase A instrument design for GECS. This TRW effort coordinated with CSU scientists actually represents the majority of the work under this project. In addition, we provide comments addressed to the Phase A instrument design study. A discussion is presented on the needed space resolution and full disk observation repeat cycle. Finally we suggest an instrument add-on to provide a redundant calibration facility.

2. *Comments on the TRW Phase A Instrument Design*

The conceptual instrument design is dependent upon details of the basic scientific goals. There are several components to the measurement of the Earth's radiation budget. Of fundamental importance is the ability to calibrate the instrument in space and track the potential time of its variation of sensitivity. Based on the experience of ERBE and CERES, the GECS detector design will show reasonable stability and that in-flight calibration will be possible. In the Phase A study, only the rudiments of the calibration equipment have been sketched. There is no engineering barrier to designing an appropriate device. Below we suggest the need for redundancy and outline a candidate system.

The spatial resolution provides the most difficult demand upon GECS. Resolutions between 16 and 50 km cross over a fundamental design break. At 50 km it would be practical to use three telescopes moving on the same scan mechanism. Each telescope would provide a different spectral component: reflected, emitted, and total. For the finer space resolution, larger telescopes would be needed. For 20 km resolution a better design would be a single telescope, with

the three different spectral sensors sharing the same optical collector. The telescope size is set by the resolution at the diffraction limit for the long-wave radiation, i.e., 50 μm . No improvement in detector sensitivity can overcome this problem.

The need for high resolution arises from the requirement to separate the scene into single surface types: clouds, clear, etc. The separation of radiation from pure scene types allows for better bi-directional adjustment from radiance to flux and to derive *cloud forcing*. We have considered this in a study of cloud types from some GOES data discussed below. This small space resolution would require detector elements smaller than planned for CERES devices. Such small detectors might pose an engineering problem, so test detectors should be built at the beginning of the next phase of the instrument design study.

The next design criteria is the need to make large scale, repetitive measurements of the upwelling radiance from the Earth. The repeat cycle for scanning the full disk viewed from the satellite can be selected at less than 2 hours. The final instrument design could make this 1 hour if necessary. Most current geosynchronous satellite climate studies utilize 3 hourly observations (e.g. the International Satellite Cloud Climatology Project). This certainly resolves the day-night variation, but it does not fully resolve the development of continental convective systems.

We think that further data studies in support of this project will *prove* the need for at least 1.5 hourly repetition. Below we discuss a short test of the time resolution problem from 24 hours of GOES data. In the candidate system, several detectors of small size and moderately fast response would be placed at the focal plan to achieve this sampling rate. Current GOES data provide accurate enough data to support a sampling study. We suggest that a Fourier analysis of a collection of half-hourly, full-disk GOES data be used to determine the minimum sampling frequency. This could be done at 32 km pixel spacing, but requires several individual full months spaced throughout the year.

In support of detailed process studies, there is a need for rapid repetition of views of small regions. Such programs like the First ISCCP Regional Experiment come to mind. The freedom to

independently control the x or y scan axes gives the means to interlace a small sector (1000 km x 1000 km) concurrently with the full disk scan. No current geosynchronous satellite can preform this rapid scan, but it is in the design capabilities of GOES NEXT. This task could be performed by the TRW concept, provided sufficient microprocessor instructions and memory are provided. This would not require moving the scan mechanism more rapidly than the normal full disk scan.

In summary, there are no barriers to fulfilling the scientific goals of the experiment with the conceptual design prepared by TRW. Specifying and building a sample detector chip should be the first part of the next phase study.

3. *Space Sampling Study*

For the derivation of radiation fluxes from the radiance measurements, the analysis scheme first identifies the scene type and then applies directional and bi-directional models to estimate flux from radiance. For the infrared, the formulae are limb darkening functions which depend very weakly on scene type. We think the difference between 20 and 40 km for the IR channel is insignificant for radiance to flux conversion.

There is a bigger problem for the reflected radiance to flux conversion because the models depend upon the cloud amount in the scene. One would prefer to have the scene contain only one surface type; cloud, ocean, desert, snow, etc. For the ERBE analysis, models were defined for 12 surface types including clear (0-10% clouds), partly cloudy (10-50% clouds), partly clear (50-90% clouds) and overcast (90-100%). As one decreases the resolution of the sensor system, the frequency of occurrence of partly cloudy or partly clear will increase and the frequency of pure scenes will decrease.

Another reason to retain as many pure scenes as possible is the segregation of the data into clear radiance and cloudy radiances. This has proven to be useful for our interpretation of the climate effects of clouds.

As a test we have set up a program to read a sample full resolution GOES visible image and compute a crude cloud amount estimation for 16, 20, 24, 28, 32, 36 km resolution detectors. The raw 1 km resolution pixels were thresholded to assign 0% or 100% cloudiness at 1 km resolution and then the frequency of occurrence of different cloud fractions was recorded for the different resolutions.

Figure 1 shows the test GOES image. This does not show the full data set because we do not have a photographic process to display 15000 pixels by 16000 pixels. As a sample, Figure 2a shows a small sector from the image at 1 km pixel resolution sampled to 4 km. Figures 2b, 2c and 2d show 4, 16, and 36 km averages of the same region with pixels replicated to make the same size output image. These show the smoothing of the larger pixels sizes. This smoothing combines clear and cloudy radiances into some intermediate radiance which appears as gray on the images. The visual impression is that bigger pixels make a much poorer product. The degradation is not as bad as it seems because our final product will be about a 100 km or larger flux estimate.

This image degradation does have a big impact if one is attempting to match radiances with surface-based radiance measurements or calculated radiances. As a secondary application of GECS, comparisons will be made with special experiments like the First ISCCP Regional Experiment or Atmospheric Radiation Measurement program of DOE. These will likely need the highest spatial and temporal resolution possible. Similarly, in comparisons with other high resolution measurements on the GEO platform, fine resolution will be very useful.

Figure 3 shows a histogram analysis of a full disk image divided into an 8 x 8 array at 16 km resolution. Figure 4 shows the opposite extreme at 36 km resolution. The 36 km regions definitely show less frequent pure scenes and more frequent mixed scenes. Figure 5 shows the differences between 36 km and 16 km. Finally, Table 1 shows the relative cloud amount frequencies of the region shown in the pictures.

Table 1. Frequency of occurrence of different cloud amounts within each pixel for different sized pixels. This area contains stratocumulus west of South America. 1990 day 298 1801 UTC GOES EAST VIS.

<u>Pixel Size</u>	<u>Cloud Amounts</u>					
	<u>0-10%</u>	<u>10-30%</u>	<u>30-50%</u>	<u>50-70%</u>	<u>70-90%</u>	<u>90-100%</u>
16 km	0.269	0.104	0.082	0.089	0.112	0.345
20 km	0.243	0.113	0.097	0.098	0.125	0.325
24 km	0.231	0.124	0.097	0.107	0.139	0.302
28 km	0.219	0.125	0.105	0.119	0.150	0.282
32 km	0.204	0.132	0.109	0.123	0.171	0.260
36 km	0.189	0.141	0.124	0.126	0.161	0.259
<u>Differences</u>						
16-36 km	0.081	-0.038	-0.043	-0.041	-0.049	0.086
20-32 km	0.039	-0.020	-0.012	-0.026	-0.046	0.064

We conclude that there is an increase in the mixed scenes from 20 km to 30 km pixels on the order of 40% to 50%. This is a substantial effect but not catastrophic for the 30 km pixels. The extra error introduced in the flux derivation could be quantified with some review of the errors in the reflection models. There remain enough clear scenes to derive clear sky forcing. These differences can not be used as a simple test to select the resolution.

4. *Time Sampling Study*

As a test of the time sampling frequency, we have looked at a set of GOES data sampled each hour for one 24-hour period. A spectral analysis was prepared for many small regions within the full disk GOES image. Figure 6 shows one image out of a sequence of 24 centered over Central America. The pixel resolution is similar to that planned for GECS. Figure 7 shows the fraction of the variance explained by the first harmonic of IR data. This is noisy because of the motion of the weather systems. Averaging this into very large regions smooths this enough to see the difference between the ocean and land areas of the images. For this quick test, the data were not remapped from image coordinates into latitude longitude, since the qualitative result is independent of the projection. Figure 8 shows many spectra giving evidence that the higher harmonics contribute a significant portion of the variance. Our opinion is that 1.5 hours sampling should be the design goal. These spectral studies need to be extended to include long time averages (weeks to a month), the visible data, different seasons, and other areas of the globe. That would be a very straightforward task for later stages of the project.

5. *NET Radiation Time Variation from Geosynchronous View: A Simulation*

To look at the time sampling problem and give a visual impression of what the instrument will view, we have prepared a video tape.¹ This simulates the radiance seen by the detector system over 5 days, sampled every 3 hours. The basic observations from the system will be the IR flux and the albedo. One can then derive the net radiation from those two analyzed numbers. The video shows a four panel image of IR flux (up positive), albedo, net radiation, and diurnal average net radiation. The diurnal average net is an estimate of the net radiation assuming that the albedo is constant for the whole day given the measurement at the instant of observation. In the original data set from ISCCP, only 5 observations of albedo were recorded, leading to the gaps in the albedo series. Of course, one can not estimate the albedo at night.

¹ The master video tape has been furnished with this report to the contract monitor at NASA, Marshall Space Flight Center, Huntsville, Alabama.

VIDEO DISPLAY

IR Flux	Reflected Flux
Instantaneous NET	Diurnal Average Net

This time loop shows the dynamic range of the fluxes and some evidence of the sensitivity to the diurnal change of albedo through the day. The largest source of variance of the fluxes is the sun angle, even larger than the presence or absence of clouds. It turns out that the atmosphere-ocean system does not respond instantaneously, but integrates the energy input over a good fraction of the day before responding. That is why we have been able in the past to get by with observations of radiation budget twice per day at some loss of accuracy.

6. *WFOV Calibration Reference*

GECS is designed to give the best time sampling possible, but only over one-fourth of the Earth. An accurate calibration facility will be included on the satellite to address the long-term stability problem. That calibration would not be performed during the earth viewing situation, but when the sensor module is turned in a special state, pointing toward a uniform calibration target. Our idea is that inclusion of a extra cavity detector staring at the full disk of the earth would provide an additional calibration reference. As a result of the Long Duration Exposure Facility mission, cavity detectors have shown very good long-term stability. A cavity detector flown on LDEF for six years showed the same sensitivity after retrieval as before launch (Hickey, 1991, personal

communication). A cavity viewing the full disk would provide a standard for comparison to the mean total scanner flux observation when it was observing the earth. Inclusion of spectral filters probably is not useful because they certainly degrade, so this cavity would just be a reference for the total GECS sensor. In addition, the view of the cavity could be arranged to provide a solar constant measurement.

The calibration problem is absolutely critical for long-term studies. We feel that some redundancy is needed if it can be accommodated. The cavity detector would provide this.

7. *Analysis Scheme*

The final analysis of the observations will require extensive use of bi-directional reflectance and emission models to convert radiance to flux or albedo. At first one can utilize the ERBE models or improved results from CERES. But as observations are accumulated, new information will be accumulated about the anisotropic character of different scene types. The challenge will be to separate the diurnal variability of the scenes from the apparent angular variability due to changing solar illumination. Considerable software will need to be developed before the launch of the satellite to take advantage of the initial data. There does not seem to be much feedback between the analysis scheme and the sensor and system design at this early stage, therefore this software development can be delayed until later in the project to take full advantage of the ERBE and CERES experience.

An additional analysis component will be the combination of GECS measurements with CERES or its successor observation system. The multiple view angles and multiple time observations of the combined experiments would provide the most accurate earth flux measurements.

8. *Conclusions*

The most important conclusion of this report is the fact that a design building upon the ERBE and CERES detector system can be utilized at geosynchronous altitude. A redesigned telescope system would be needed. First order time and space sampling studies indicate that measurement repeat cycles of 1.5 hours and space resolution near 20 km would be useful for monitoring the Earth's radiation budget. These are possible with the TRW Phase A design. Exact design specifications require more extensive sampling studies and construction of sample detectors.



Figure 1. GOES full disk image sampled to 32 km resolution.

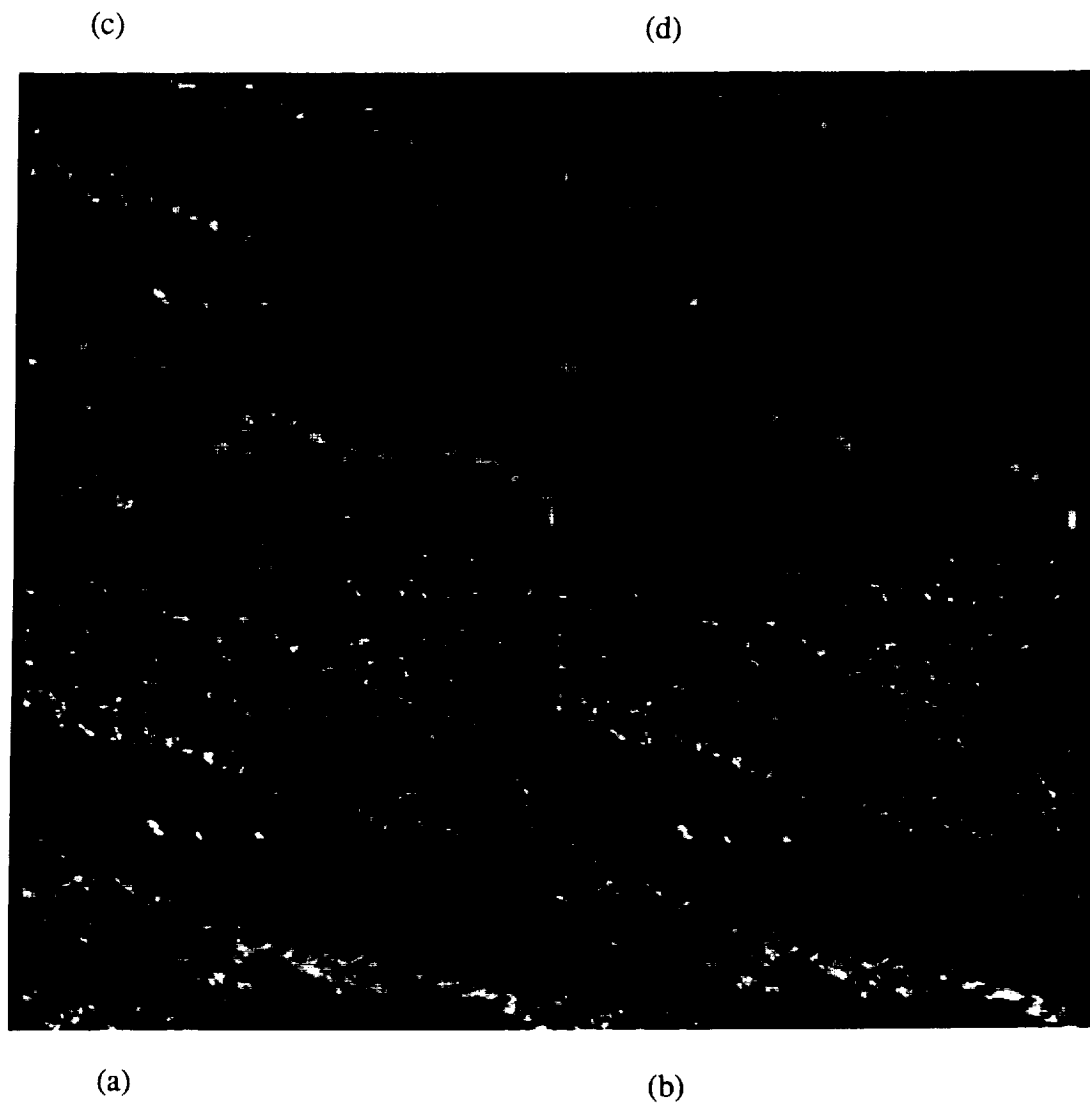


Figure 2. Small region: (a) sampled to 4 km resolution from 1 km pixels; (b) averaged to 4 km resolution; (c) averaged to 16 km resolution; and (d) averaged to 36 km resolution.

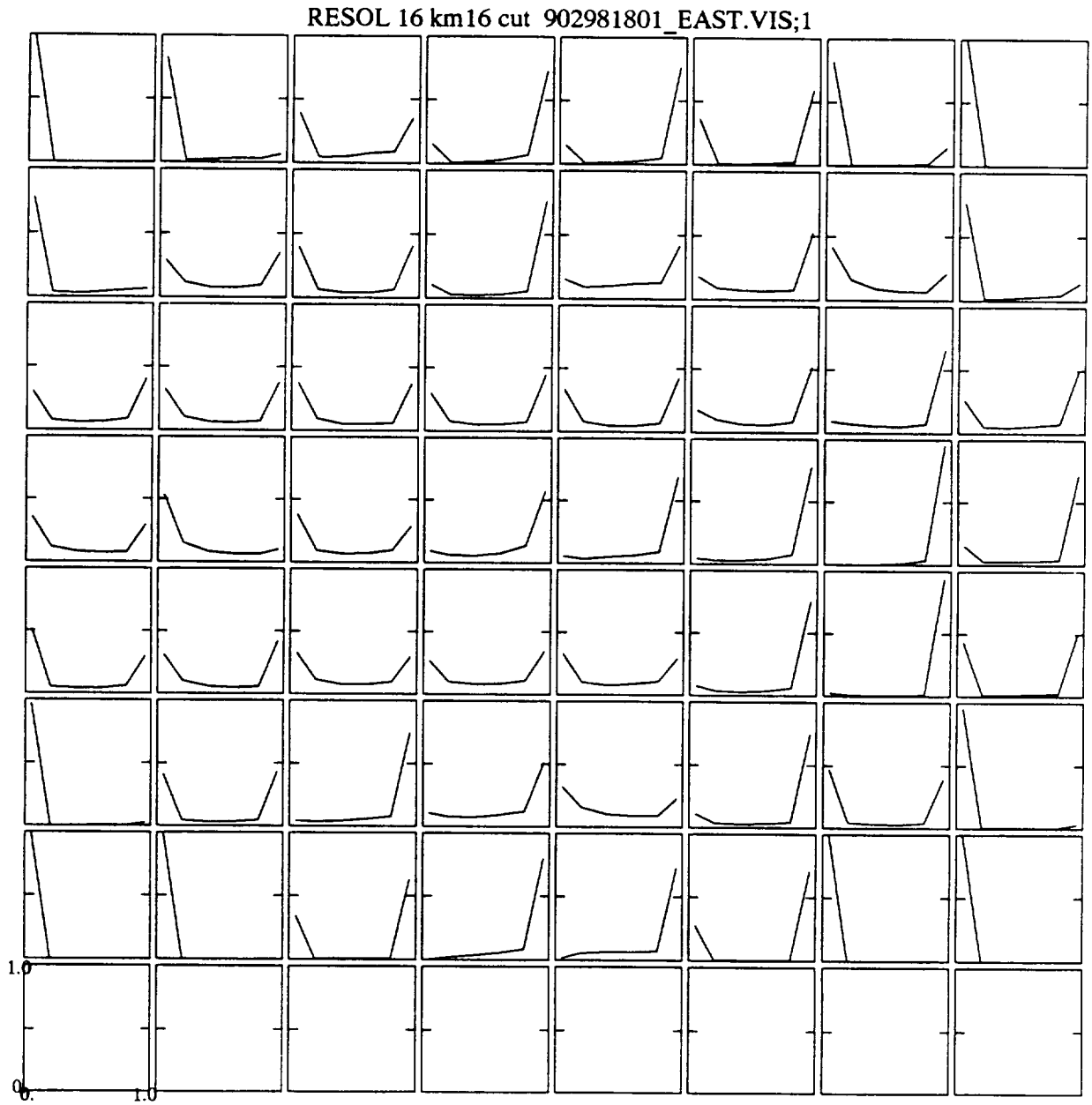


Figure 3. Histograms of cloud frequencies from 16 km pixels.

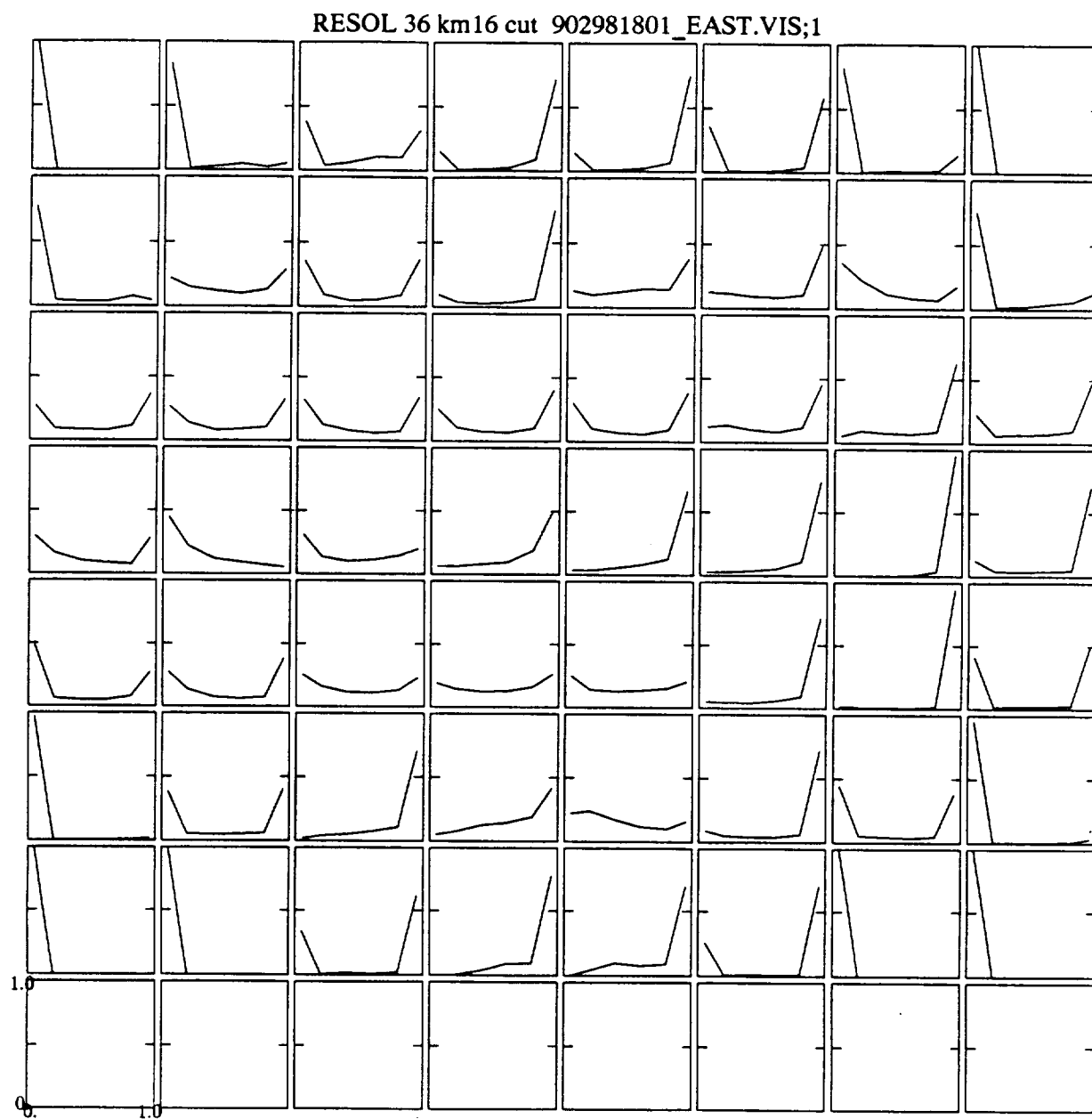


Figure 4. Histograms of cloud frequencies from 36 km pixels.

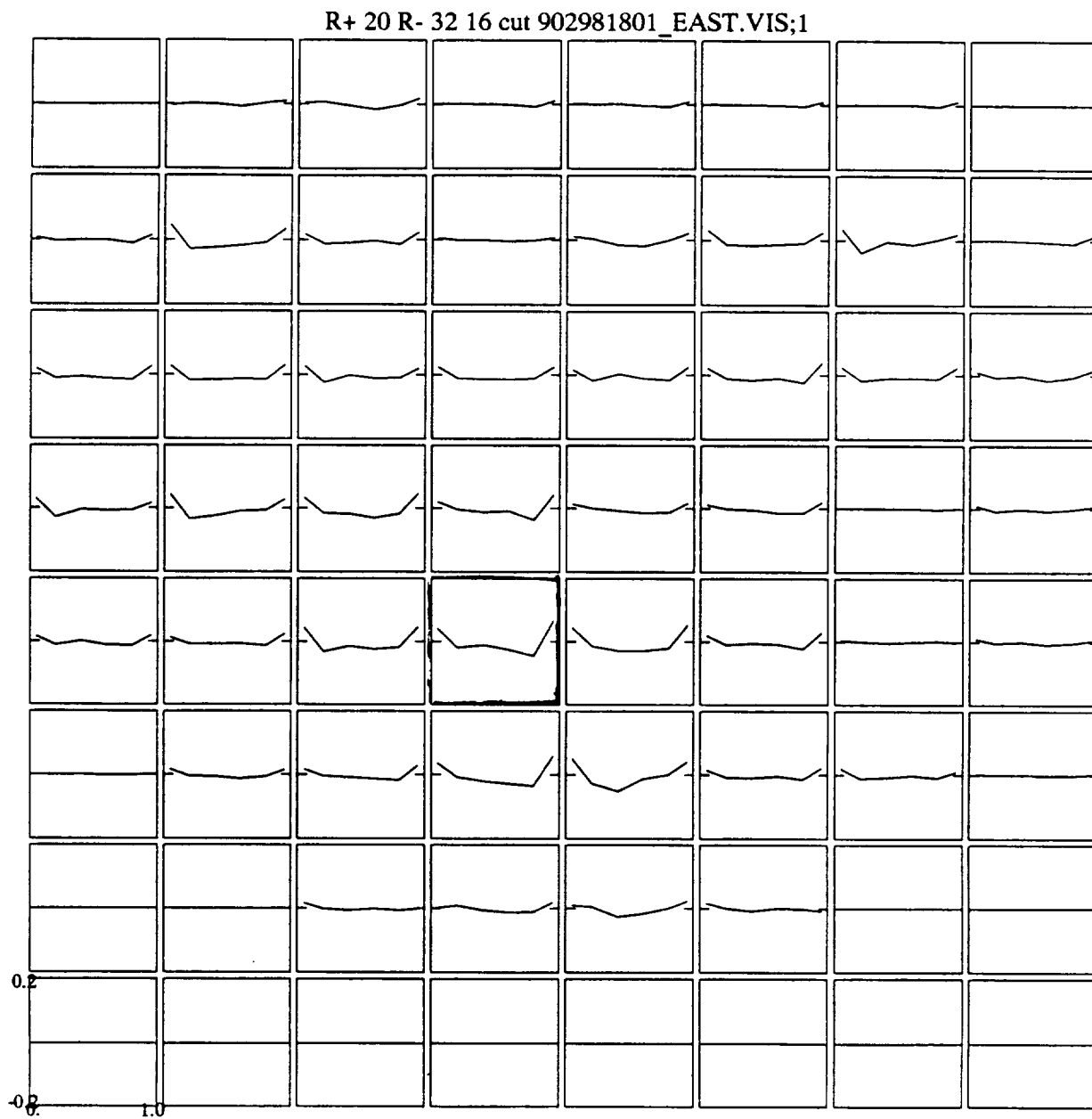


Figure 5. Differences in frequencies between 20 km and 32 km pixels.



Figure 6. Image of region analyzed for time spectral.

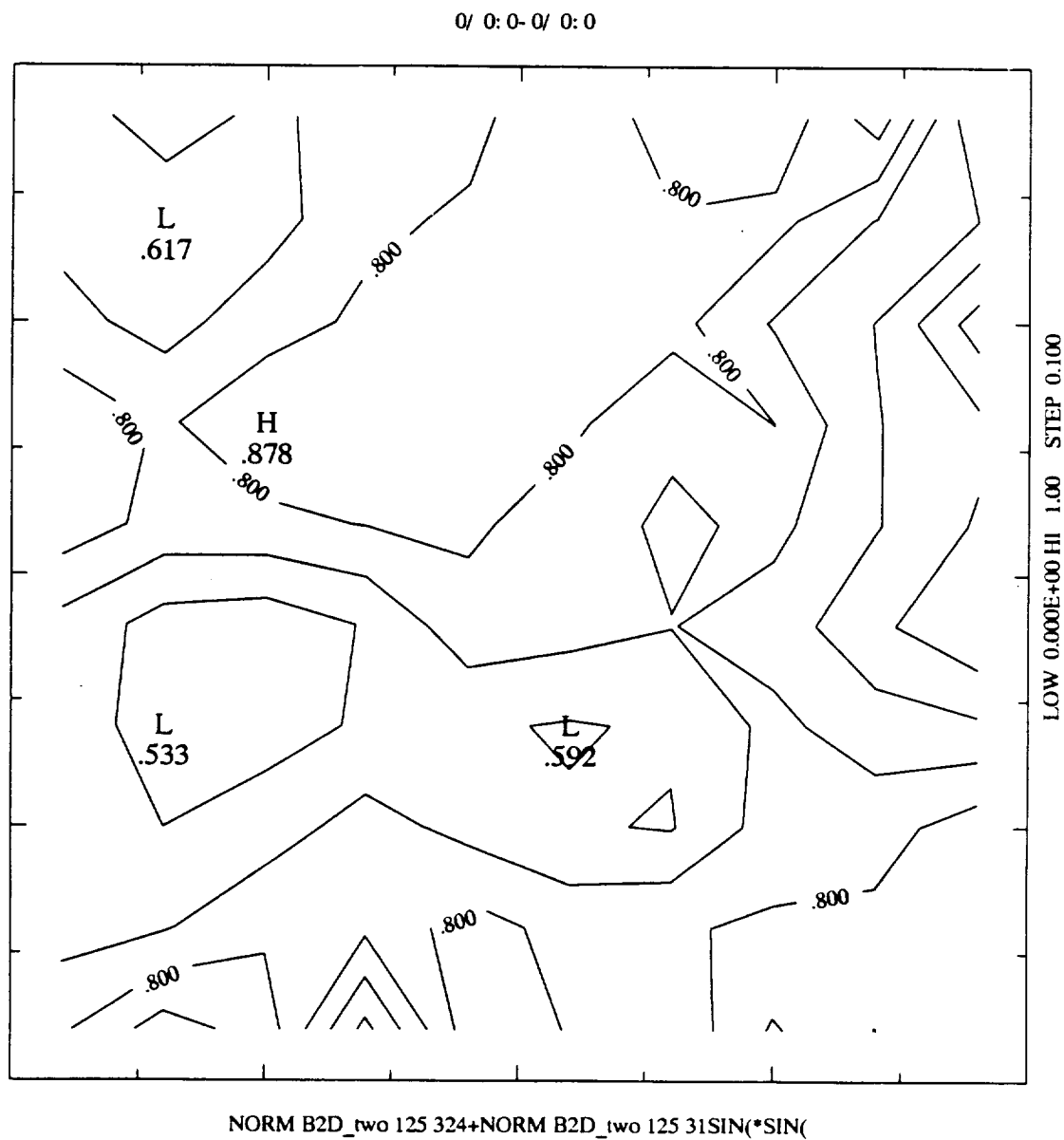


Figure 7. Amplitude of the first harmonic of 24 hours of GOES IR data. This is noisy because only one day contributed.

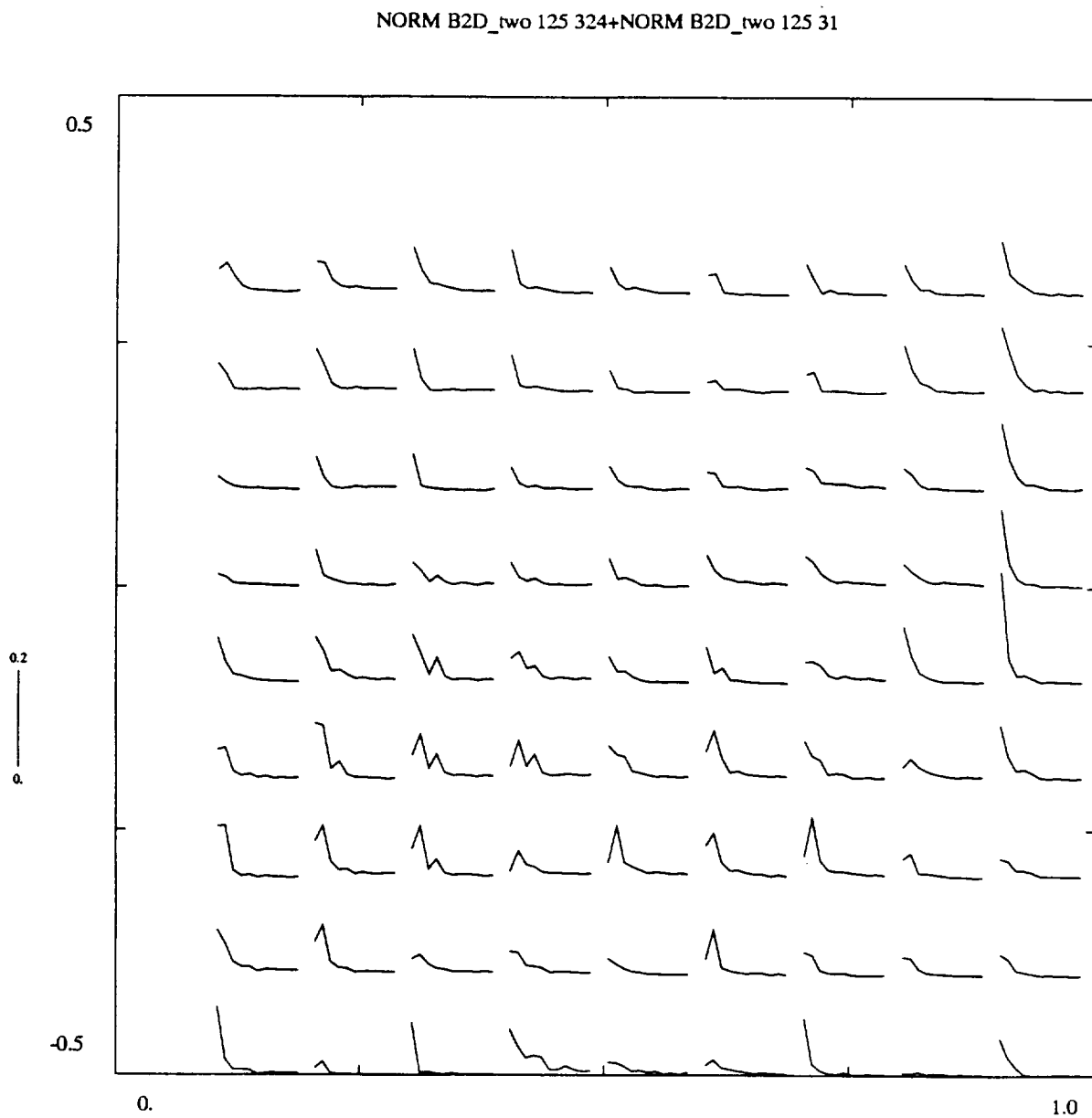


Figure 8. Many spectra of the GOES IR from data sampled at 1 hour intervals. Only the second through twelfth harmonics were plotted. The spectra are normalized to show the variance explained for each location.



Geostationary Earth Climate Sensor

GECS Phase A Final Report

**February 6, 1991
Revision N/C**

**Prepared for:
Colorado State University
Fort Collins, Colorado 80523
Contract No. G-1938-1**

**Prepared by:
TRW Applied Technology Division
Space and Technology Group
One Space Park
Redondo Beach, California 90278**

REVISION/CHANGE RECORD

FOR DOCUMENT NO. GECS-A

[illegible]

Table Of Contents

	Page
1.0 INTRODUCTION	1
1.1 Scope	1
1.2 Objectives	1
1.3 Guidelines	2
2.0 STUDY APPROACH	6
3.0 SYSTEM TRADES	11
3.1 Optical Design	17
3.2 Detector Selection	18
3.3 Electronics Subsystem	18
3.4 Pointing Subsystem	19
4.0 SIZE, WEIGHT, POWER SCALING	34
5.0 CALIBRATION	42
6.0 PHASE B RECOMMENDATIONS	43

List of Figures

Figure #	Title	Page
1-1	SOW Study Guidelines	4
1-2	ERBE/CERES Experience	5
2-1	Three Telescopes/Nadir Mount	8
2-2	Three Telescopes/Side Mount	9
2-3	Single Telescope/Nadir Mount	10
3-1	10 km System Trades	21
3-2	20 km System Trades	22
3-3	30 km System Trades	23
3-4	50 km System Trades	24
3-5	Coverage Trades	25
3-6	Aperture vs FOV	26
3-7	Point Design Summary	27
3-8	Optical Design Criteria	28
3-9	Two Mirror Cassegrain	29
3-10	Four Mirror GECS Design	30
3-11	Detector Selection	31
3-12	GECS Electronics	32
3-13	Derived Pointing Requirements	33
4-1	Instrument Size/Single Telescope	36
4-2	Instrument Size/Three Telescopes	37
4-3	Instrument Mass	38
4-4	Instrument Power	39
4-5	Telemetry Rate/Single Telescope	40
4-6	Telemetry Rate/Three Telescopes	41

1.0 INTRODUCTION

1.1 Scope

This document provides the final report on the Geostationary Earth Climate Sensor (GECS) Phase A design study. This study has examined the idea of configuring an earth radiation budget instrument, such as ERBE/CERES, for operation at geosynchronous range. Such a platform offers some unique opportunities, as well as some very challenging problems. The desire to maintain spatial resolution similar to that achieved with the CERES design (20 to 30 km), while operating at a range some fifty times greater, necessitates significant changes in the optical subsystem. These modifications are developed via the general approach described in Section 2.0 of this report. Section 3.0 presents the detailed system trades, followed by a discussion of each of the major subsystems examined during Phase A. Section 4.0 presents an instrument size, weight, power model which is scaled to telescope aperture. This model is used with the system trades presented in Section 3.0 to tie instrument size, weight, power to key performance parameters such as spatial resolution, earth disc coverage time, and noise equivalent radiance.

Section 5.0 discusses calibration of the GECS instrument. It is expected that GECS calibration techniques will borrow directly from proven ERBE/CERES approaches, with specific engineering considerations for the larger GECS aperture.

The last section (Section 6.0) presents recommendations for the Phase B definition study. This section identifies key technical/engineering issues that merit particular consideration in any subsequent effort.

1.2 Objectives

The purpose of this study is to determine the performance

capabilities of a geosynchronous-based earth radiation budget instrument. Quantitative trades are established between key system parameters including spatial resolution, noise equivalent radiance, and earth disc coverage time. Instrument size, weight, power, and telemetry requirements are determined as a function of these parameters and used to constrain instrument design options by host vehicle capabilities.

1.3 Guidelines

This study effort is directed by guidelines provided in the Statement of Work (SOW), technical interchange with the members of the review team (CSU, LaRC, and MSFC), and ERBE/CERES experience. Requirements extracted from the GECS SOW are summarized in Figure 1-1. The spectral response ranges cited here are slightly different than those specified for CERES. The shortwave limit (for the Total and SW channels) is 0.3 μm for CERES vs. 0.2 μm in the GECS SOW. The longwave limit for the LW (broadband option) and Total channels for CERES is 50 μm vs. a goal of 100 μm for GECS (50 μm is stated as being acceptable for GECS if the 100 μm limit becomes a design driver). The break between SW and LW is also slightly different for CERES. The upper limit on the SW channel is 3.5 μm , and the lower limit on the LW channel (broadband option) is 5.0 μm . The GECS SOW specifies 4.0 μm for both of these values. These differences were discussed with the GECS review team members and it was agreed that the CERES numbers should supersede those in the SOW. It was also agreed that GECS should assume the broadband option (5 to 50 μm) for the LW channel vs. the window option (8 to 12 μm) now being considered for CERES.

Technical discussions with the review team also established some refined values for the Noise Equivalent Radiance (NER) and spatial resolution requirements. The upper limit for NER was revised downward from 1.5 to 0.6 $\text{W}/\text{m}^2\text{-sr}$ and an upper limit of 30 km was established for the spatial resolution. The trade space presented in this report extends well beyond these requirements

bounds, however, the point designs presented are fully compliant with these revised values.

The design options presented in this study are heavily influenced by ERBE/CERES experience. Key factors are summarized in Figure 1-2. These factors include radiometric accuracy, scene radiance sampling parameters (spatial overlap, zero radiance reference, channel-to-channel temporal sampling requirements), and instrument size, weight, power, and lifetime guidelines. The ERBE/CERES experience also supports this study in many of the detailed design trades such as detector selection, mirror coating choice, signal processing, calibration, etc.

Geostationary Earth Climate Sensor

SOW Study Guidelines

Parameter	Requirement
Spectral Response	As flat as possible
Channel 1 (SW)	0.2 to 4.0 μm
Channel 2 (LW)	4.0 to 100 μm
Channel 3 (Total)	0.2 to 100 μm
(LW cut-off may be reduced to 50 μm if a design driver)	
Field-of-View	0.3 to 1.0 mrad (10.8 to 35.9 km)
Noise Equivalent Radiance	0.3 to 1.5 $\text{W}/\text{m}^2\text{-sr}$
Earth Disc Coverage Time	1 to 3 hours
In-Flight Calibration	To be provided
Recloseable Cover	To be provided on telescope(s)

Figure 1-1

Geostationary Earth Climate Sensor

ERBE/CERES Experience

Parameter	Requirement
Radiometric Accuracy	
Channel 1 (SW)	$0.5 + 0.01 * P_{sw} \text{ (W/m}^2\text{-sr)}$
Channel 2 (LW)	$0.75 + 0.005 * P_{lw} \text{ (W/m}^2\text{-sr)}$
Channel 3 (Total)	$0.5 + 0.005 * P_{tot} \text{ (W/m}^2\text{-sr)}$
Spatial Sampling	
In-Flight Radiance Reference	Minimum 0 to 25% Overlap
Temporal Sampling	Space Look Simultaneous viewing
Dimensions:	
Length x Width x Height	0.6 x 0.5 x 0.7 meter 23.6 x 19.7 x 27.6 inches
Weight	45 kg
Power	45 Watts
Lifetime	5 years

Figure 1-2

2.0 STUDY APPROACH

This study was conducted in three phases. The first phase commenced in late July 1990 and established the global trades between performance (NER, coverage time, spatial resolution) and instrument size, weight, and power as scaled to instrument aperture. A point design was developed assuming a three telescope configuration with a single detector element per telescope. Performance capabilities were determined for an instrument package that met the size, weight, and power constraints for a CERES instrument. Mechanical layouts for this point design are shown in Figures 2-1 and 2-2. Figure 2-1 shows an instrument configuration assuming a location on the nadir face of the host platform. Figure 2-2 demonstrates the simpler support structure that is possible if the instrument is located on the host platform side (velocity or anti-velocity). These system trades and the initial point design were presented to CSU and MSFC representatives in mid-September at TRW. The review package was also provided to team members at LaRC for their review. This marked the conclusion of this first phase of the study.

Initial comments from the review team focussed on improving the spatial resolution of the design. This performance consideration had been compromised (50 km resolution) in the interest of achieving a compact instrument package. The second phase of the study examined design cases that would provide 30 km or better spatial resolution. These designs retained the three telescope configuration, but utilized multiple (three) detector elements to improve NER at a given disc coverage rate (or to provide higher coverage rate at a given NER). Aperture dimensions were determined based on practical limits for telescope focal ratio ($f/1$) and detector width (0.1 mm), along with the desired spatial resolution (20 to 30 km). These design options were discussed with the review team in mid-October via a four-way teleconference involving CSU, LaRC, MSFC, and TRW. This conference resulted in

some recommendations for the final phase of the study. First, it was requested that the aperture be sized to reduce the diffraction blur at 50 μm . The system design studies performed in the initial phase had demonstrated that diffraction could significantly increase the system resolution at longer wavelengths. This could produce an instrument point spread function that had strong dependence on wavelength. This potential impact was assessed by members of the science team, and the recommendation made that the diffraction blur at 50 μm be no greater than the geometrical spatial resolution. It was requested that systems meetings these criteria and providing spatial resolutions of 20 and 30 km be examined. It was noted that achieving the 20 km spatial resolution under these conditions would necessitate an aperture of more than 20 cm. It was agreed that for this point design, a single telescope configuration would be developed. The results of these final Phase A design options are detailed in Section 3. A mechanical layout of the single telescope approach is shown in Figure 2-3.

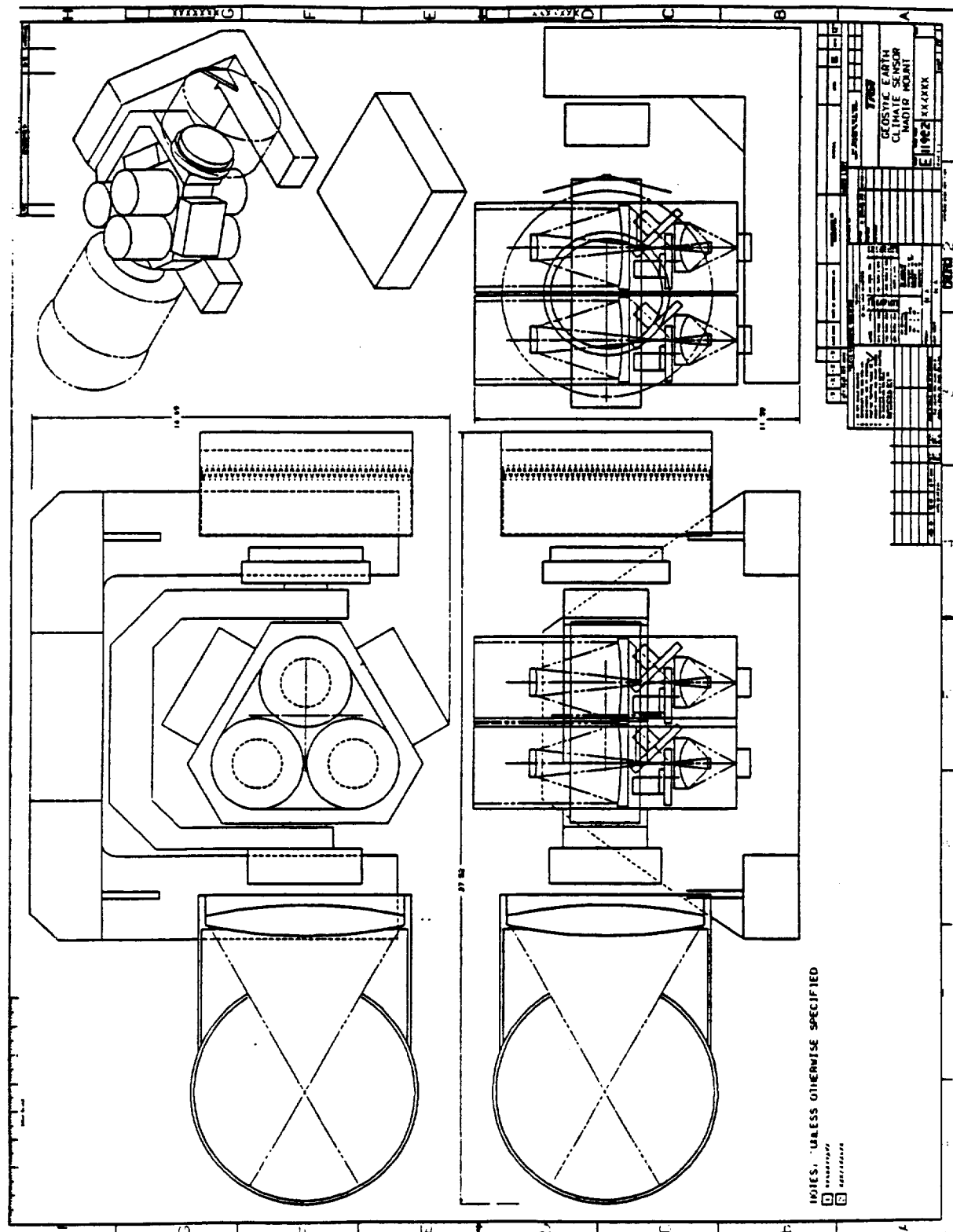


Figure 2-1

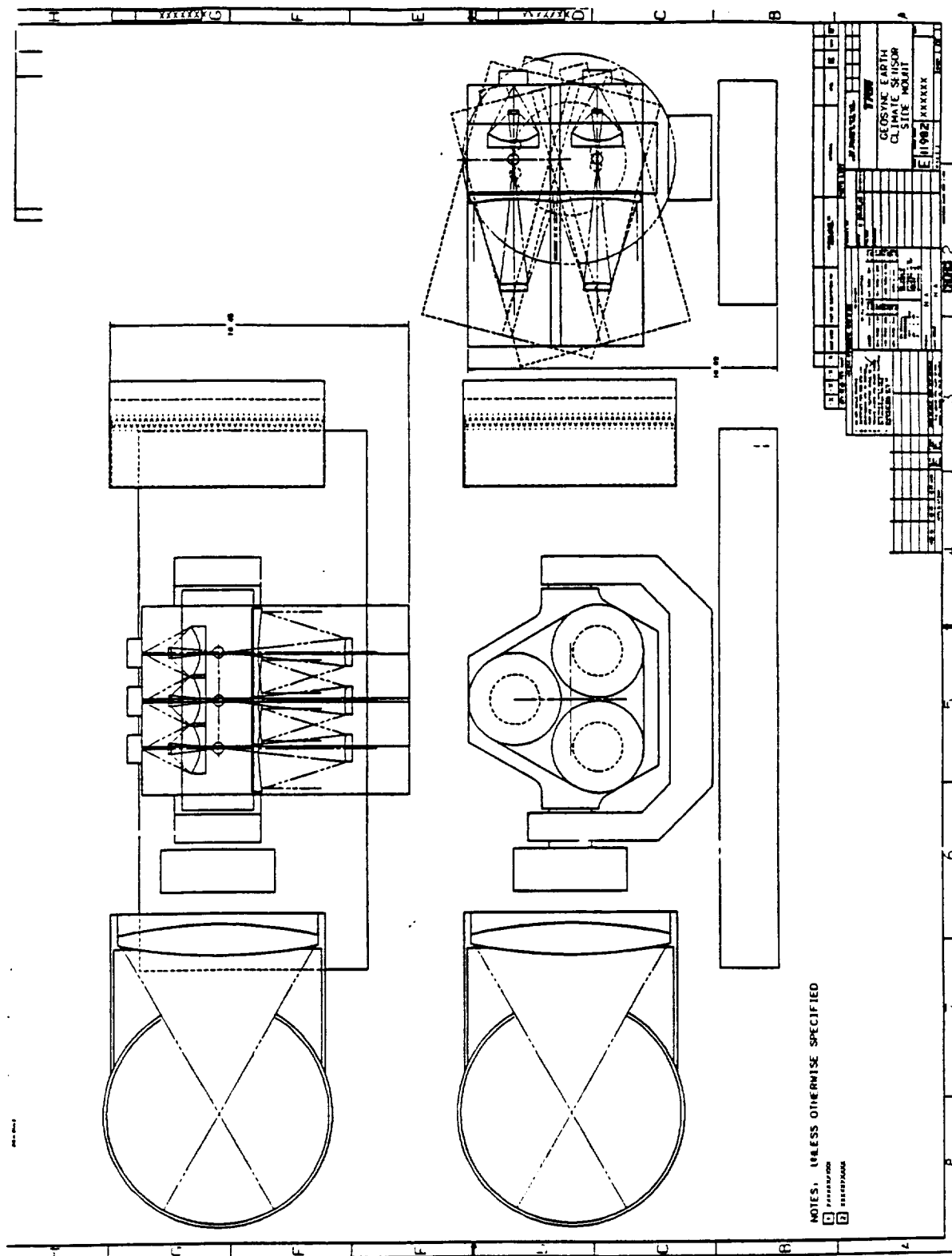


Figure 2-2

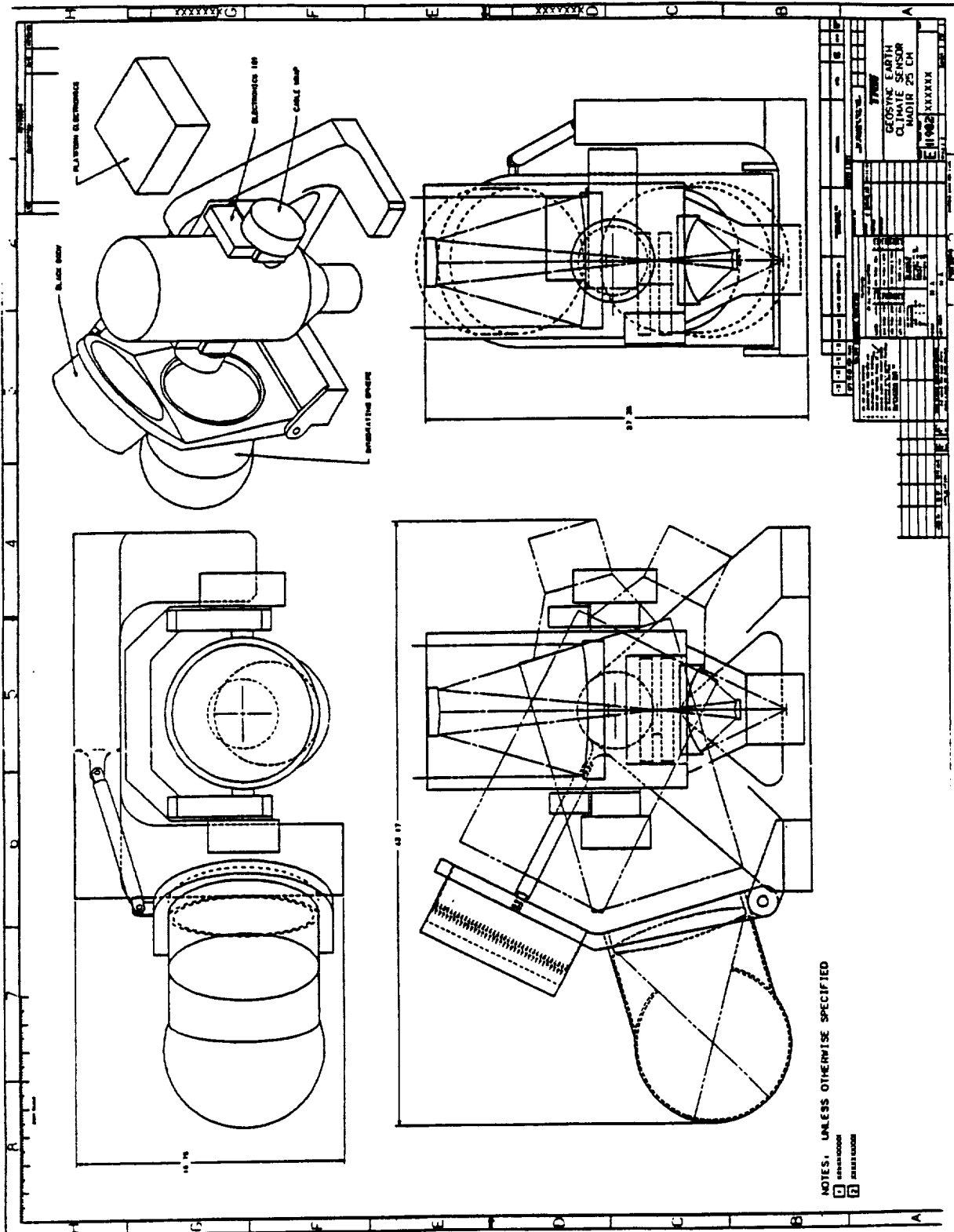


Figure 2-3

3.0 SYSTEM TRADES

At the system level, this study has concentrated on developing quantitative relationships between Noise Equivalent Radiance (NER), spatial resolution, and Earth disc coverage time. Wherever possible, these trades are presented without ties to specific hardware or component performance, and are based on first-order principles. However, in order to tie detector noise power (NEP) to signal bandwidth, it becomes necessary to employ a detector model that relates NEP to detector dimensions and signal bandwidth. For this study, the performance data for the CERES thermistor bolometer were scaled appropriately as determined from the subcontractor's (SERVO) data. This is consistent with the detector selection for GECS discussed in Section 3.2.

Development of the system performance relationships begins with the basic equation for NER:

$$(1) \quad \text{NER} = \text{NEP} / (T_o * A * \text{OMEGA}_T) \quad (\text{W/m}^2\text{-sr})$$

Where: NER = Noise Equivalent Radiance (W/m²-sr)
 T_o = Optics Transmission (w/ obscuration)
 A = Aperture Area (m²)
 OMEGA_T = FOV Solid Angle (sr)
 NEP = Detector Noise Equivalent Power (W)

Note that the telescope FOV (OMEGA_T) can be expressed in terms of ground resolution:

$$(2a) \quad \text{OMEGA}_T = (\text{GNDRES})^2 / R^2 \quad (\text{sr})$$

Where: GNDRES = Pixel Footprint (km)
 R = Orbit Range (km)

Or in terms of telescope parameters:

$$(2b) \quad \text{OMEGA}_T = (w_d/fl)^2 = [w_d/(D * f\#)]^2 \quad (\text{sr})$$

Where:

- w_d = Detector Width (m)
- fl = Telescope Focal Length (m)
- D = Telescope Diameter (m)
- $f\#$ = Telescope Focal Ratio

Incorporating Equation (2a) in Equation (1), and noting that $A = \pi D^2/4$, yields the relationship between ground resolution and NER:

$$(3) \quad \text{NER} = 4 * \text{NEP} * R^2 / (\pi * \text{GNDRES}^2 * D^2 * T_o) \quad (\text{W/m}^2\text{-sr})$$

Figure 3-1a plots this relationship for 10 km ground resolution using a range (R) of 35873 km (geosynchronous orbit) and an optics transmission (T_o) of 0.5 (based on ERBE/CERES experience). This relationship is also plotted for ground resolutions of 20, 30, and 50 km as shown in the 'a' panels of Figures 3-2 through 3-4. These plots allow one to readily determine the required aperture to achieve a specified NER for a given ground resolution and detector noise power (NEP). Once the aperture is determined, the telescope focal ratio ($f\#$) can be determined as a function of detector dimensions using the relationship derived from Equations (2a) and (2b):

$$(4) \quad f\# = w_d * R / (\text{GNDRES} * D)$$

This relationship is plotted in the 'b' panels of Figures 3-1 through 3-4. Common x-axis scaling between the 'a' and 'b' panels in these figures allows one to easily assess the relative impact of varying aperture on NER performance and telescope requirements. In order to establish particular design points, detector size and NEP must be determined. Experience with thermistor bolometer from ERBE and CERES Phase 1 activities provide a first-order model of detector NEP as a function of detector width, time constant, and operating bandwidth:

$$(5) \quad \text{NEP} = C * w_d * \text{bw} / \text{tau} \quad (W)$$

Where:

C = Scale factor based on CERES experience = $1.136\text{E}-9$
 bw = Bandwidth
 tau = Bolometer time constant

This relationship is plotted in Figure 3-5a as $\log (\text{NEP})$ vs bandwidth for various detector sizes. A time constant of 4 msec is used as a nominal value, again based on CERES experience. This plot is used in conjunction with the plot shown in Figure 3-5b to relate detector NEP to Earth disc coverage time. A reasonable estimate of the system bandwidth required to support the mission may be derived knowing the telescope solid angle and the disc coverage time:

$$(6) \quad \text{bw} = \text{OMEGA}_E / (\text{OMEGA}_T * T * 60)$$

Where OMEGA_E = Earth disc solid angle
 T = Disc coverage time (min)

Using equation (2a) to express OMEGA_T in terms of ground resolution and solving for T yields =

$$(7) \quad T = \text{OMEGA}_E * R^2 / [60 * \text{bw} * (\text{GND RES})^2] \text{ (min)}$$

Note that this calculation assumes a single detector element and simultaneous viewing in the three (LW, SW, Total) channels. Results (disc coverage time) for other configurations can be readily determined by scaling (multiplying) the y-axis of Figure 3-5b by the number of sample periods required to collect LW, SW and total data (typically one or three as established by the number of telescopes) divided by the number of detector elements per telescope. A three telescope system employing three detector elements per telescope therefore achieves coverage times one-third

of those presented in Figure 3-5b. If the three detector elements are retained, but a common telescope is used, coverage time is again as shown in the figure as the improvement provided by the additional elements is offset by the need to make sequential measurements in the three bands.

Figure 3-5 can be used with Figures 3-1 through 3-4 to explore countless design options. Typically, these options are evaluated by using the desired ground resolution and coverage time to establish the necessary system bandwidth from Figure 3-5b. The bandwidth and detector width next determine the detector NEP (Figure 3-5a). In general, it is best to select as small a detector as possible, with a practical limit of 0.1 mm as determined by manufacturing/processing capabilities of potential suppliers (SERVO). Having determined the detector NEP, the next step is to size the telescope aperture using this NEP and the required NER. Figure 3-1a, -2a, 3a or -4a is used, as determined by the ground resolution requirement, to determine the necessary aperture diameter to achieve the NER requirement. Once the aperture is established, the 'b' panel of the same figure is used to determine the telescope f#, using the detector width previously established.

One additional consideration must be addressed in these design trades. Because GECS endeavors to achieve similar performance (spatial resolution, NER) to that proposed for CERES, while at considerable greater range, a much smaller FOV is required. At the longwave end of the LW and total channels, diffraction blur can become sizeable compared to the geometric FOV. The diffraction blur (full angle) is:

$$(8) \quad \text{BLUR} = 2.44 * \text{LAMBDA}/D$$

Where:

$$\text{LAMBDA} = \text{LW limit} = 50 \text{ um}$$

$$D = \text{telescope diameter (m)}$$

This blur can be compared (ratioed) to the geometric FOV to establish a figure of merit (BETA) for diffraction:

$$BETA = BLUR/FOV$$

$$(9) \quad BETA = 2.44 * LAMBDA * R/[D * (GND RES)]$$

Note that equation (9) can be solved for D, thereby providing a direct determination of the telescope aperture as a function of ground resolution and diffraction requirements:

$$D = 2.44 * LAMBDA * R/[BETA * (GND RES)]$$

This relationship is plotted in Figure 3-6 for various values of BETA with LAMBDA = 50um. Discussions with the review team established a requirement of BETA = 1 at 50 um, therefore this curve can be used to establish the required aperture for the point designs discussed at the end of Section 2.

The first of these designs is required to provide 30 km resolution with a three-telescope, three detector element per telescope configuration. From Figure 3-6, the aperture requirement is determined as 15 cm. From Figure 3-3a, the corresponding NEP for a 0.6 W/m²-sr NER performance level with a 15 cm is about 3.5 E-9 W (log (NEP) = -8.456). This establishes the maximum NEP requirement for the detector that supports system performance of 0.6 W/m²-sr. A minimum size requirement for the detector can be established using Figure 3-3b.

Preliminary optical analysis has demonstrated that a focal ratio (f#) of 1.0 is as fast as should be considered. Employing this limit, a lower limit on the detector size is set at about 0.125 mm.

Detector NEP/size trades are also tied to disc coverage time as previously shown in Figure 3-5. Disc coverage time is optimized

when system bandwidth is maximized. This occurs when the detector NEP requirement is satisfied with zero margin and the minimum detector size is used. This point ($\log(\text{NEP}) = -8.456$, 0.125 mm) can be plotted on Figure 3.5b and used to establish the corresponding system bandwidth (about 26Hz). This bandwidth along with the ground resolution (30 km) lead directly to the disc coverage time capability from Figure 3-5a (about 22 minutes).

Figure 3-5 can also be used to establish best-case NEP performance based on a maximum disc coverage time requirement. For example, a 1 hour (60 minute) requirement for a 50 km resolution system results in a bandwidth requirement of about 10Hz. This 10Hz bandwidth coupled with the minimum detector size of 0.125 mm produce an NEP of about $1.8\text{E}-9$ W ($\log(\text{NEP}) = -8.75$). The lowers the NER of the system from 0.6 to less than $0.4 \text{ W/m}^2\text{-sr}$.

A similar approach is used for assessing the second point design (20 km ground resolution, single telescope, three detector elements). From Figure 3-6, the minimum aperture required is 22cm. Since a single telescope is used in this point designs, moderate size, weight, and power can be retained while choosing a somewhat larger aperture than this minimum. A aperture of 25 cm was selected as providing some margin with respect to the minimum required, while retaining a telescope package size smaller than that needed for the three-telescope, 20 km system. The 25 cm aperture results in a maximum detector NEP requirement ($\text{NER} = 0.6\text{W/m}^2\text{-sr}$) of $4.6 \text{ E}-9$ ($\log(\text{NEP}) = 8.333$ and a minimum detector size of 0.14 mm ($f\# = 1.0$). These parameters lead to a maximum system bandwidth of about 33Hz, which provides a disc coverage time of 118 minutes. This example illustrates one of the key disadvantages of the single telescope approach. Because the LW, SW, and total measurements must be made sequentially, disc coverage time suffers dramatically. Operation at higher bandwidth can recover coverage time, but at the expense of higher NER. If neither NER and coverage time are compromised, then the telescope

requirements are driven to unacceptable values ($\sim 35 - 40$ cm aperture, $f\# \sim 0.75$).

Key parameters for these point designs are summarized in Figure 3-7. Discussions regarding the various subsystems are provided in the following sections.

3.1 Optical Design

The design criteria for the GECS optical subsystem are summarized in Figure 3-8. Note that the geosynchronous platform produces some driving requirements that steer the GECS design away from that used for ERBE/CERES. The faster focal ratio ($f\# = 1.0$), plus the need to provide space in the optical train for a filter wheel and/or chopper, make the simple two-mirror Cassegrain design used previously unacceptable (see Figure 3-9). For GECS, a four mirror design, shown in Figure 3-10, was developed to satisfy these additional constraints. This design provides ample room for a chopper and/or filter if required, and achieves the required focal ratio (1.0) with simple optics (parabolic primary, the rest are spheres). The design has been analyzed for performance over field angle to determine the potential for using multiple detector elements at the focal plane. The detailed Code V results are included in Appendix A. This analysis has demonstrated that the optical design performance (blur circle) is well within that due to diffraction for field angles that accommodate three detector elements. Effort that might be considered for Phase B activities would include an investigation of design performance vs field angle as the complexity of the optical surfaces is allowed to increase.

The only disadvantage with the proposed design that has been identified, is the impact of the two additional (with respect to ERBE/CERES) mirror surfaces on the spectral response of the instrument. The nominal mirror coating for GECS is proposed to be silver, as is planned for CERES (ERBE used aluminum). While silver avoids the major dip in reflectivity that aluminum exhibits at

about 0.8 μm , it does not extend as far into the ultraviolet. The four surfaces used in the GECS design will tend to amplify this short-coming. Discussions with the review team produced a general agreement that the silver coatings were still a superior choice, however, this issue may merit additional investigation during Phase B of this study.

3.2 Detector Selection

The factors considered in the GECS detector selection process are summarized in Figure 3-11. The over-riding requirement for this aspect of the design is the broad spectral response (0.3 to 50 μm). Only a few detector types, including cavity, pyroelectric, and thermistor bolometer, meet this requirement. Of these options, only the thermistor bolometer has demonstrated performance satisfying GECS requirements. Bolometer performance on the ERBE mission has been shown to be extremely stable over five years of in-flight operation. While the dimensions of the devices required for GECS (0.1 to 0.2 mm) are considerably smaller than those used for ERBE (2 mm), device manufacturing of these sizes is routine and has been discussed with the CERES bolometer supplier (SERVO).

Perhaps, the best argument for continued use of the thermistor bolometer for GECS is the lack of evidence for a viable alternate. Candidates that might theoretically perform as well (active cavity detectors, pyroelectric detectors) require additional development and therefore, represent significant technical risk.

3.3 Electronics Subsystem

The GECS Electronics subsystem will be virtually identical to that used for ERBE/CERES. This subsystem performs the following functions (see Figure 3-12):

- a) Command Processing
- b) Mode Sequencing
- c) Gimbal/Pointing Control
- d) Temperature Control (Detectors/Blackbody)

- e) Signal Conditioning
- f) Experiment/Housekeeping Data Acquisition
- g) Telemetry Formatting
- h) Power Conditioning

The GECS electronics design will benefit directly from designs produced for ERBE and CERES. Functions such as temperature control, signal conditioning, gimbal control, and data acquisition can use previously developed circuit designs with only minor modifications. The processor architecture including the basic approach for performing the command processing, mode sequencing, and telemetry formatting functions can also be taken from existing designs, however, significant effort will be required to tailor these functions to specific host platforms and operational scenarios.

3.4 Pointing Subsystem

The most demanding pointing requirements for instruments of this type (which have performed their missions from low earth orbit) have historically been driven by the ground track velocity of the host platform. Coverage is achieved by scanning from limb to limb in a direction perpendicular to the velocity vector while the spacecraft proceeds along its orbit. This cross-track scan must be of sufficiently high rate to reach an extreme angle above the limb (space-look for zero radiance reference), then reverse and retrace to the nadir position in the amount of time it takes for the telescope FOV to progress about 70% of its own length. This is necessary to provide adequate spatial sampling of the scene. For a FOV of 30 km and a ground track velocity of about 7 km/sec, this means the instrument must scan some 150 degrees in less than 3 seconds. Allowing about 0.5 seconds for dwell at the extreme angle (space look), results in an earth scan rate of about 60 degrees per second. This scan rate then drives the detector sampling rate requirement, which in turn establishes the system bandwidth.

For GECS, the geosynchronous platform removes orbital dynamics from the first-order calculations of the scan rate requirements. Since the platform remains essentially fixed with respect to the scene, the factors that drive the sample rate, and ultimately the scan rate, become somewhat more discretionary. The sample rate for GECS, as discussed in Section 3.0, is derived directly from the ground resolution and the disc coverage time. The disc coverage time is selected based on a subjective assessment of the scene dynamics (cloud motion, lighting conditions, etc.). The use of disc coverage time to drive these trades may be considered somewhat arbitrary, but is used here to address SOW requirements. Additional study may conclude that regional studies at higher temporal sampling rates are more representative of nominal instrument observations.

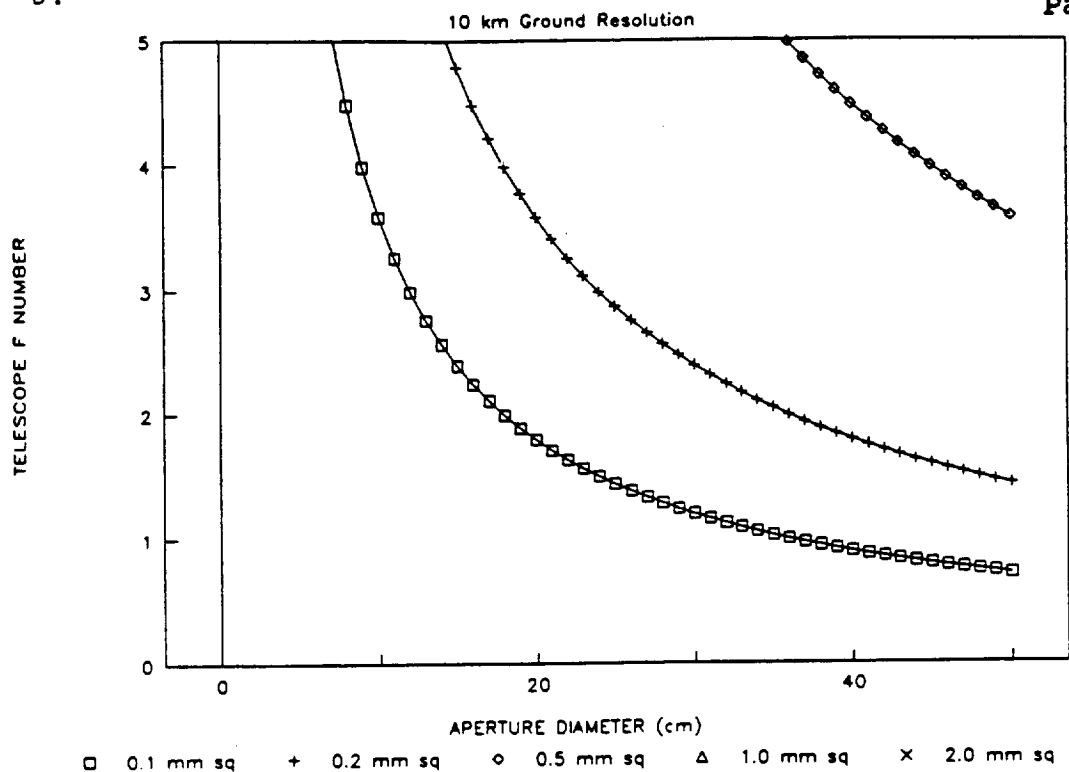
Typical GECS scan rate requirements can be readily derived for the point designs discussed in Section 3.0. These designs produce signal bandwidths of 26 and 33 Hz for the 30 and 20 km systems, respectively. The required scan rate can be approximated by the ground resolution (converted to an angular dimension) divided by the sample period (the reciprocal of the bandwidth). Values of 1.25 and 1.06 degrees/second are obtained for the 30 and 20 km systems, respectively. Note that because these rates are much lower than those required for instruments such as ERBE or CERES, the required acceleration for GECS is also much lower. This tends to counter the higher GECS telescope inertia when calculating the torque ($T = J * \alpha$) required to support the GECS scan profile. Motors of size, weight, and power consumption characteristics similar to those used for ERBE and CERES are therefore appropriate for the GECS design as well. These results are reflected in the size, weight, power trades discussed in Section 4.0.

A summary of the derived pointing requirements for GECS is presented in Figure 3-13.

B.

GECS F NUMBER TRADES

Page 21



A.

GECS NOISE EQUIVALENT RADIANCE TRADES

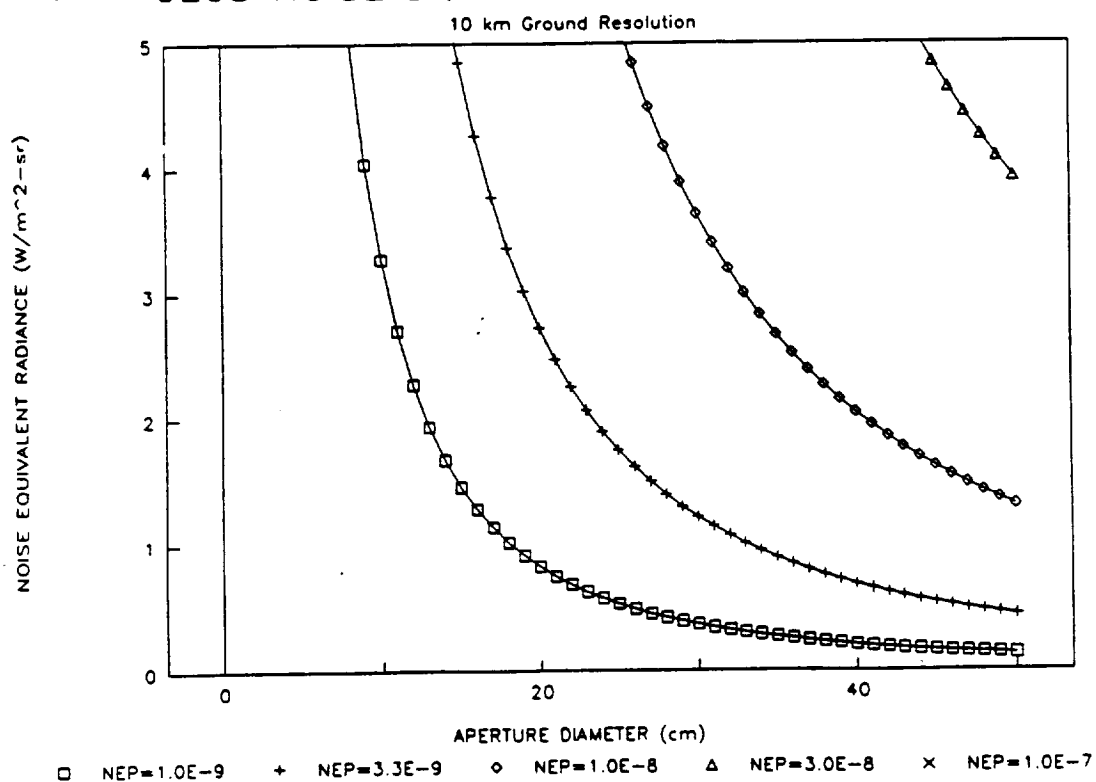
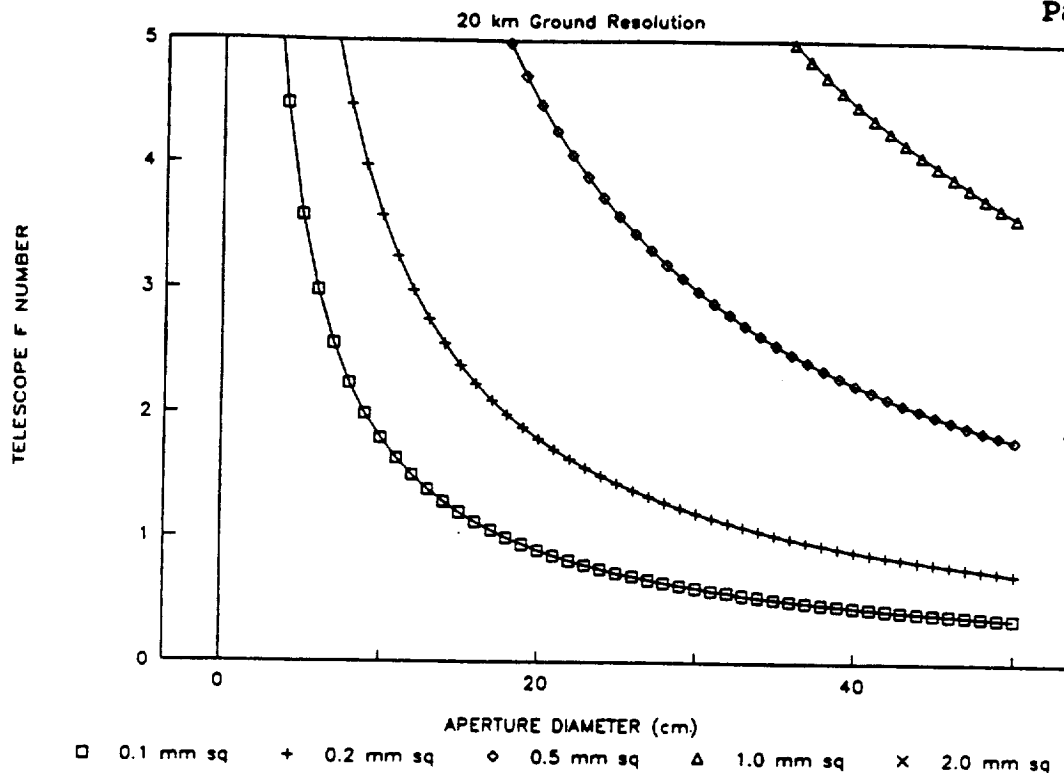


Figure 3-1

B.

GECS F NUMBER TRADES

Page 22



A.

GECS NOISE EQUIVALENT RADIANCE TRADES

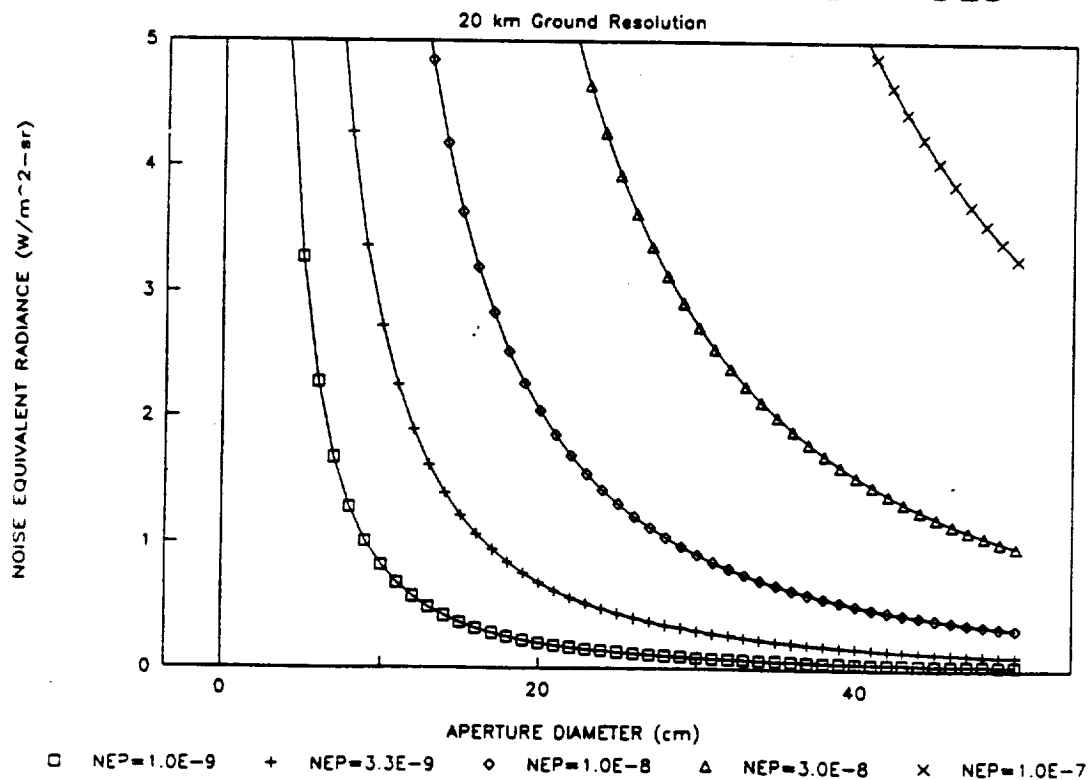
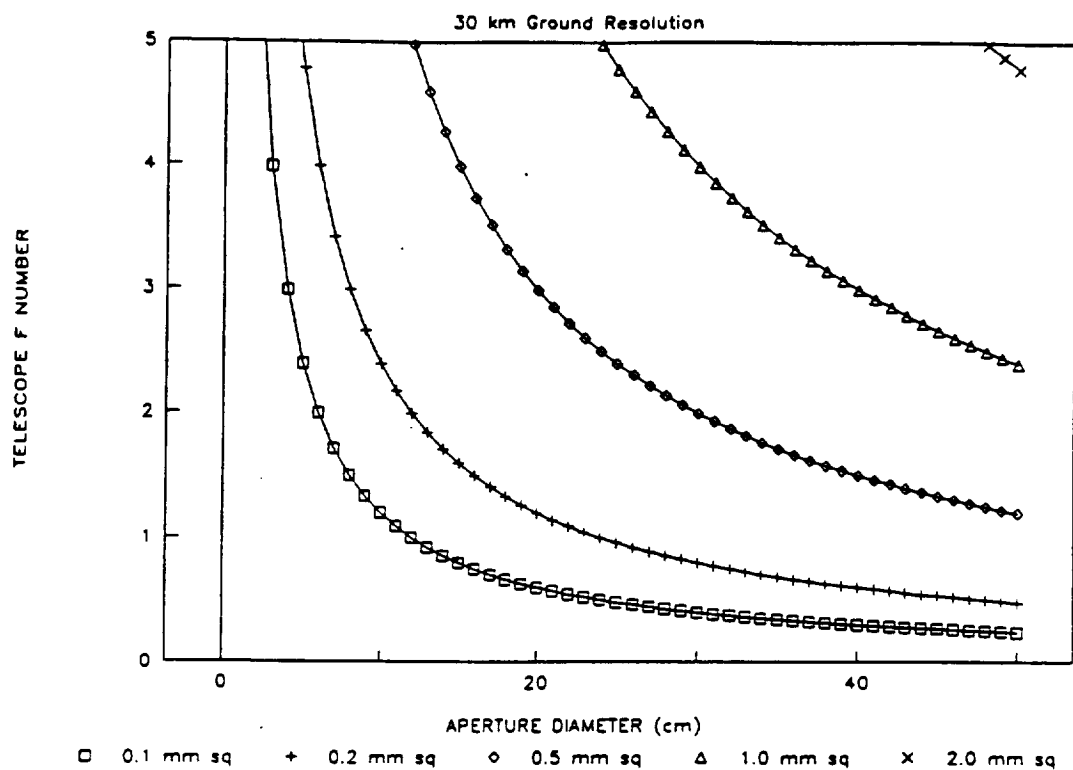


Figure 3-2

B.

GECS F NUMBER TRADES

Page 23



A.

GECS NOISE EQUIVALENT RADIANCE TRADES

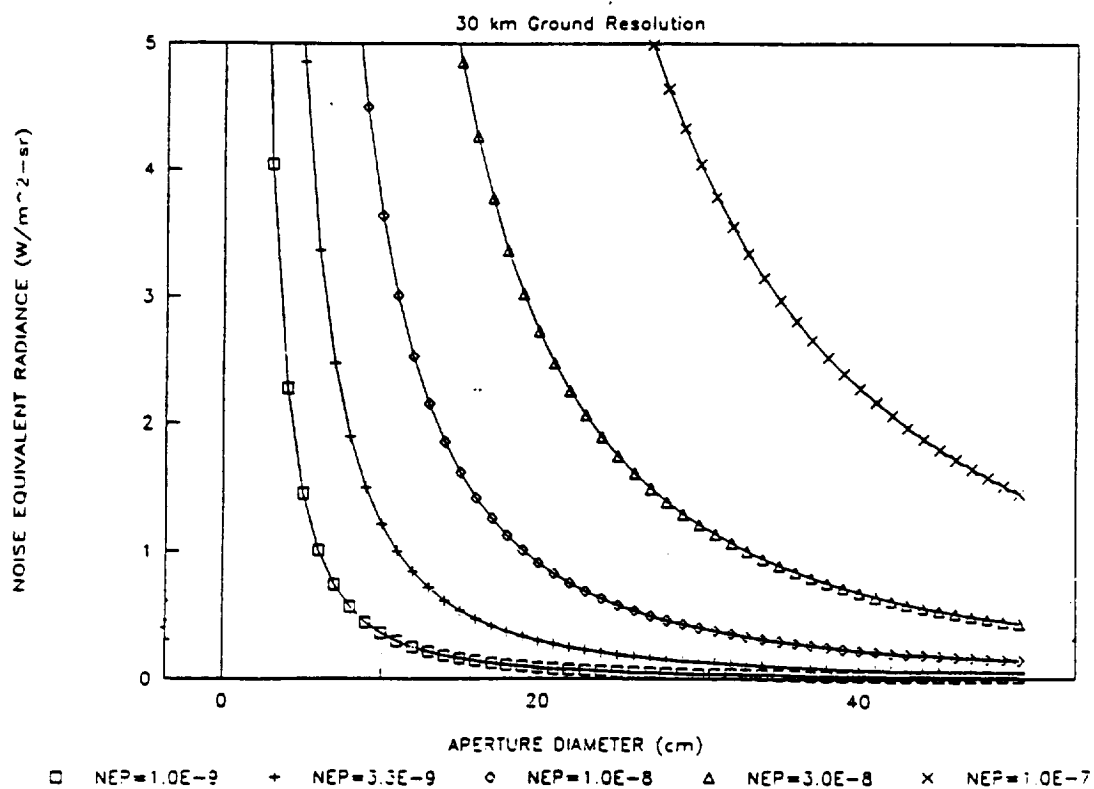
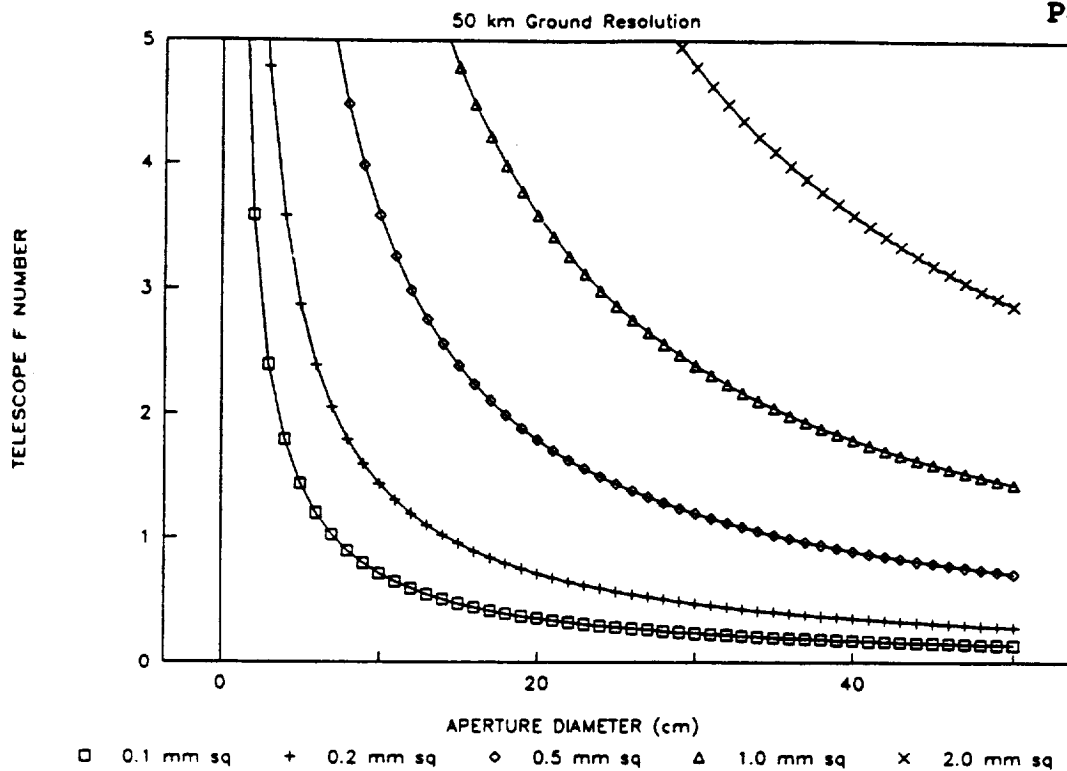


Figure 3-3

B.

GECS F NUMBER TRADES

Page 24



A.

GECS NOISE EQUIVALENT RADIANCE TRADES

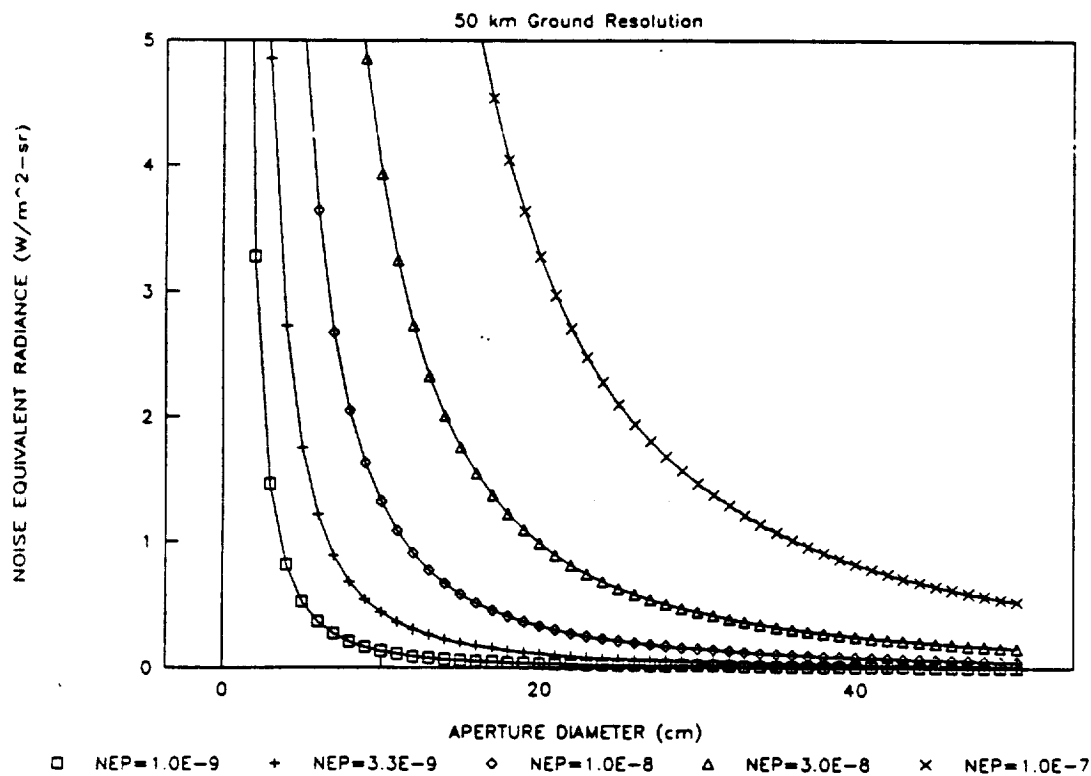
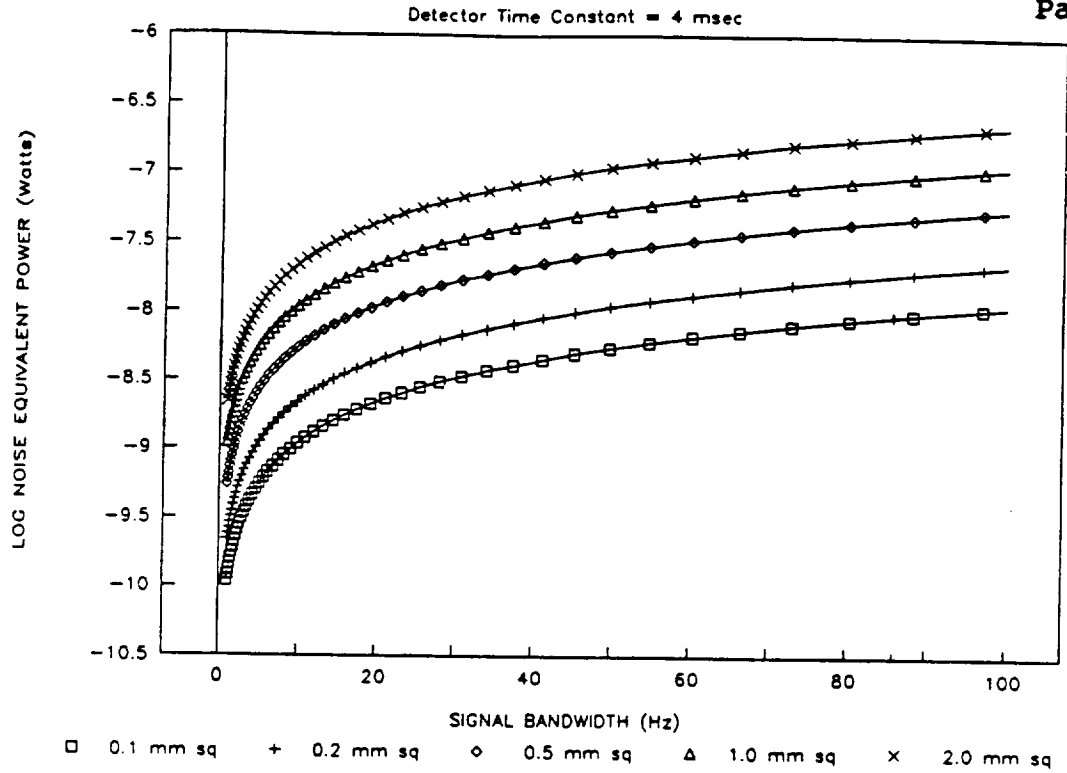


Figure 3-4

B.

GECS SIGNAL BANDWIDTH TRADES

Page 25



A.

GECS COVERAGE TIME TRADES

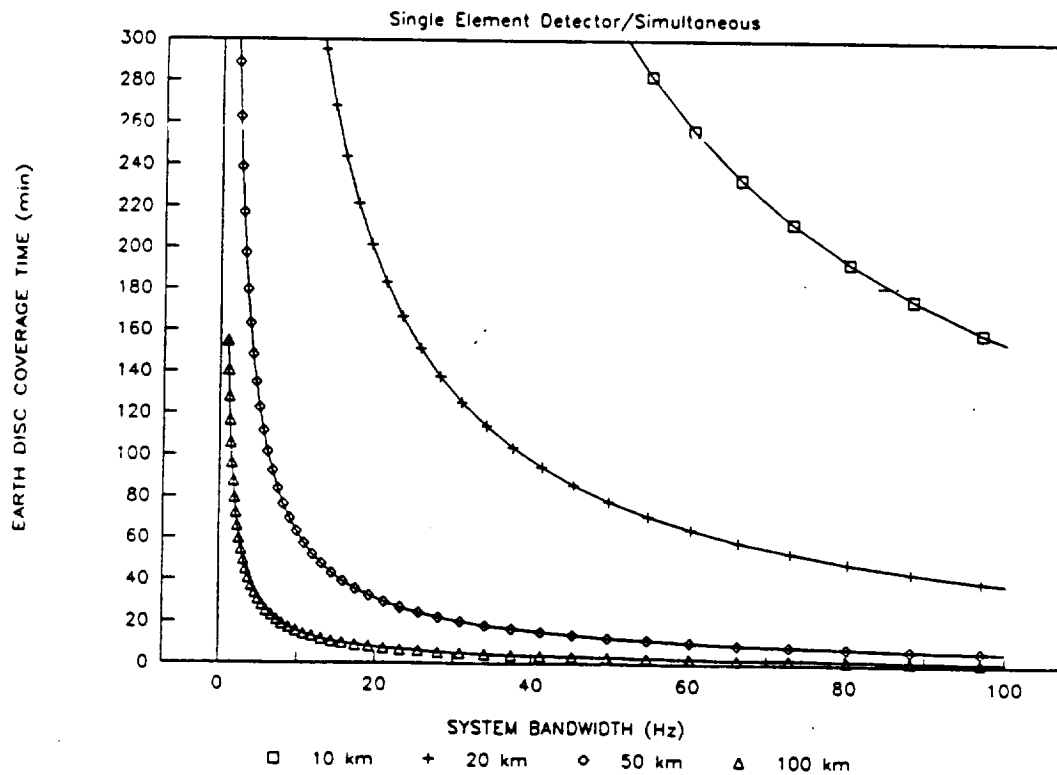


Figure 3-5

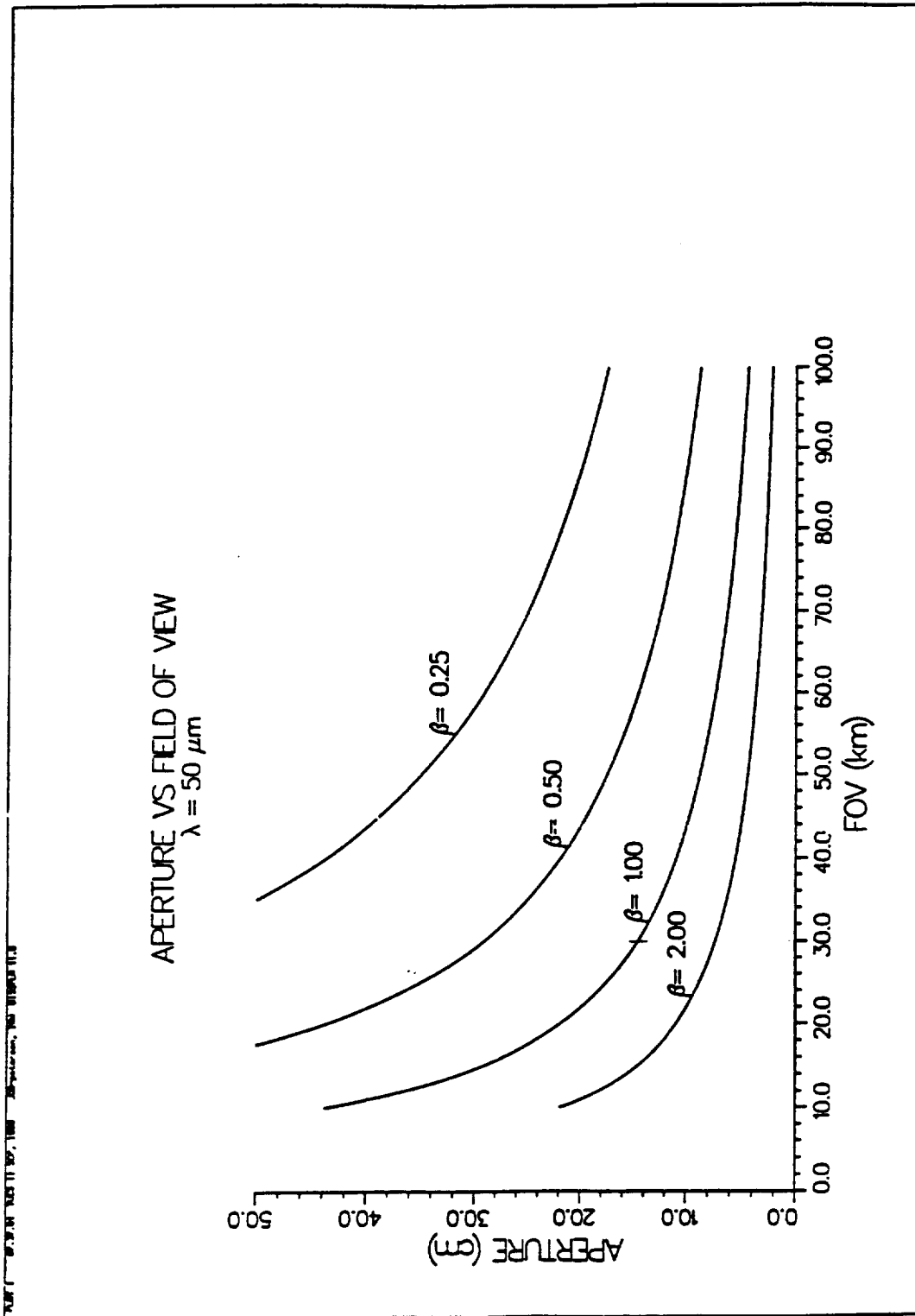


Figure 3-6

Geostationary Earth Climate Sensor

Point Design Summary

Parameter	Point Design	
	30 km	20 km
Aperture (cm)	15	25
Coverage Time (min) (@ 0.6 W/m ² -sr, f#=1.0)	22 (bw=26Hz)	118 (bw=33Hz)
Noise Equivalent Radiance (W/m ² -sr) (min @ f#=1.0)	0.4 (@ T=1hr, bw=10Hz)	0.4 (@ T=3hr, bw=22Hz)
Detector Size (mm)	0.125	0.140
Max NEP (Watts) (log(NEP))	3.5x10 ⁻⁹ (-8.456)	4.6x10 ⁻⁹ (-8.337)

Figure 3-7

GECS Optical Design Criteria

- Optical system should be fast ($f/1$ if possible) to reduce overfilling of detector at long wavelengths and minimize detector size.
- $0.3 \mu\text{m} < \lambda < 50 \mu\text{m}$
- Need room for filters, choppers, etc.
- Prefer simple, less expensive mirrors (i.e. spheres, parabolas) to minimize cost and risk.
- Obscuration should be small to avoid aggravating diffraction blur at the detector and maximize throughput.
- Tolerances must be reasonable.

Figure 3-8

Two Mirror Cassegrain Design Used for ERBE and CERES Does Not Work for GECS

- Complicated (expensive) mirrors:
 - f/0.25 parabola primary
 - hyperboloid secondary
- Little or no room for choppers or filters.
- Tolerances?

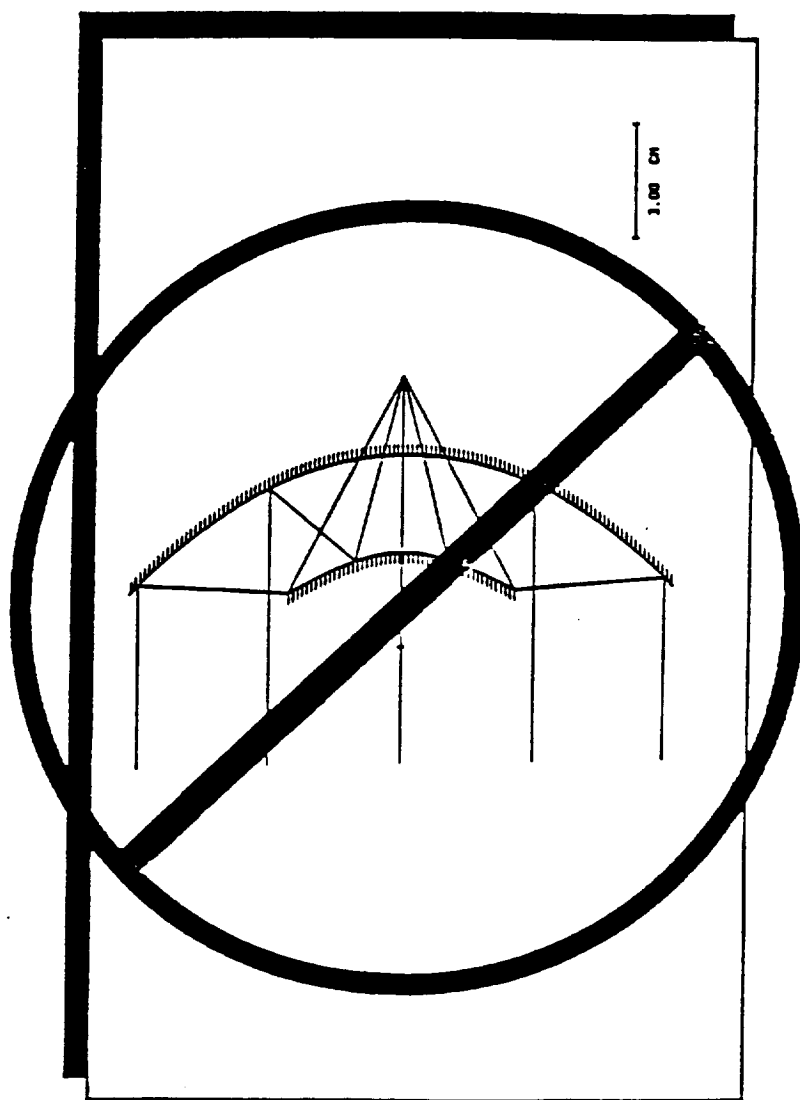


Figure 3-9

A Four Mirror Design that Meets General Requirements

Simple Optics:

- 3 Spheres
- 1 Parabola

Fast ($f/1$) system

Small obscuration (12%)

Room for filters, chopper, etc.

Tolerances reasonable

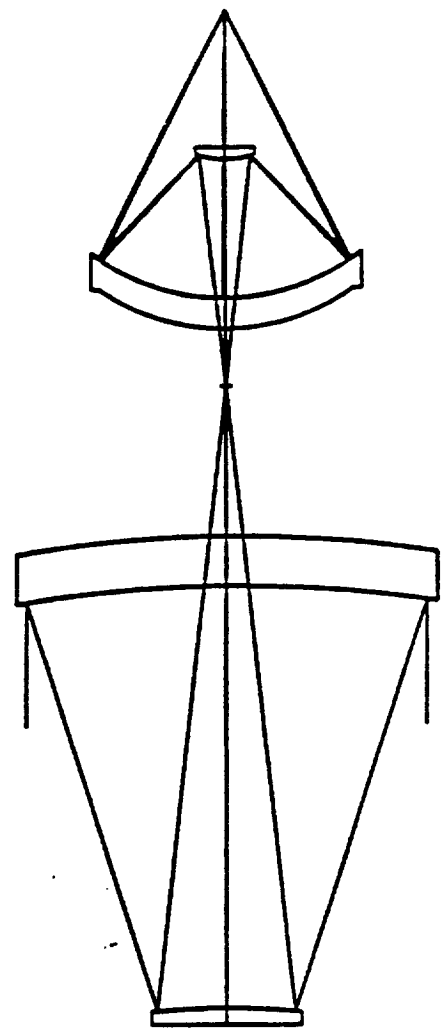
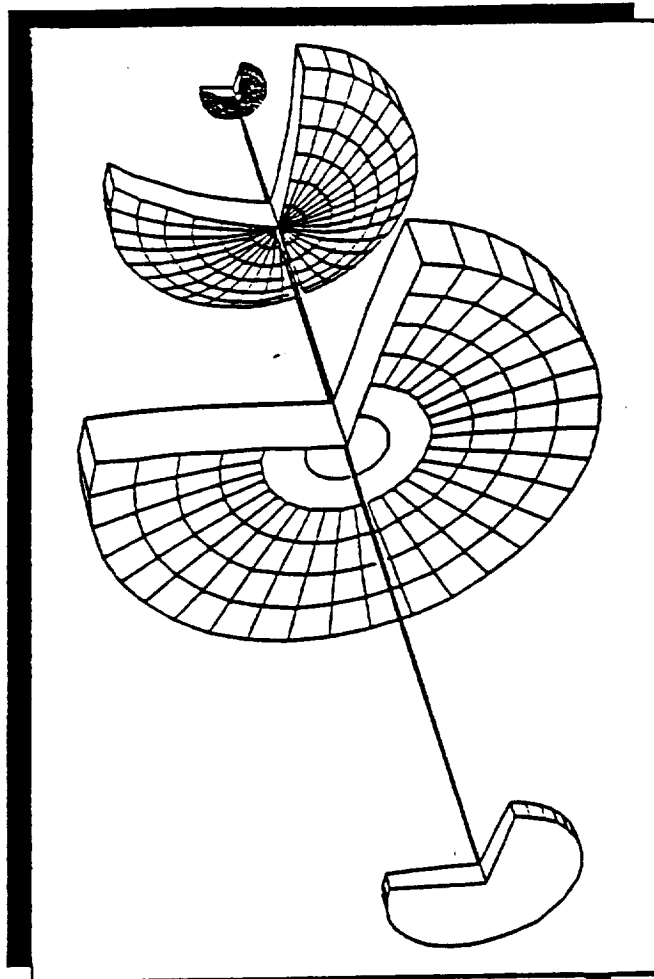


Figure 3-10

Geostationary Earth Climate Sensor

Detector Selection

Continued use of thermistor bolometer detectors provides the best link to previous Earth Radiation Budget data.

- o On-orbit stability of thermistor bolometers demonstrated by ERBE Scanners.
- o Smaller detector dimensions afforded by GECS design results in devices with lower noise power.
- o Alternate detector types have major disadvantages:
 - Cavity detectors have excessively high noise power unless cryo-cooled.
 - Array detectors can not provide the required spectral response without multiple focal planes.
 - Pyroelectric detectors were examined for CERES and rejected due to difficulty of manufacture.

Figure 3-11

GECS ELECTRONICS

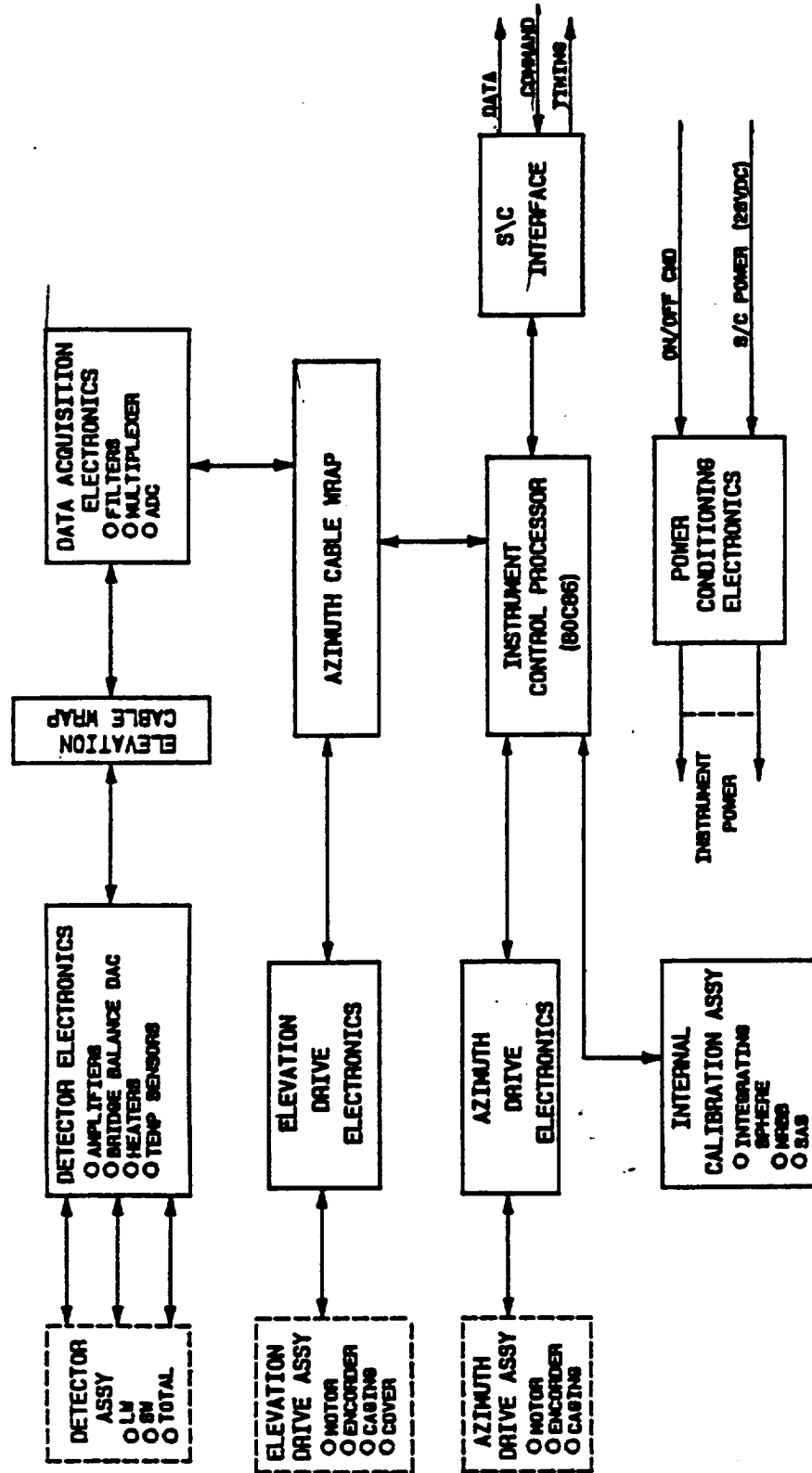


Figure 3-12

Geostationary Earth Climate Sensor

Derived Requirements

Parameter	Requirement
Gimbal Range	
Earth Scan	
Azimuth	+/- 15 Degrees
Elevation	+/- 15 Degrees
In-Flight Calibration	
Azimuth	+/- 90 Degrees
Gimbal Scan Rate	
Earth Scan	2 Degrees/sec
In-Flight Cal Scan	10 Degrees/sec
Pointing Knowledge (20 km FOV)	25 urad

Figure 3-13

4.0 SIZE, WEIGHT, POWER SCALING

Dimensional scaling of the GECS instrument is shown in Figures 4-1 and 4-2 for the single and three telescope configurations, respectively. The length and width dimensions are defined by the outer dimensions of the instrument bench, which are scaled directly from the outer diameter of the telescope assembly (one or three telescopes). The overall instrument height is scaled from the individual telescope diameter and assumes a focal ratio of 1.0.

Weight scaling for both single and three telescope configurations are shown in Figure 4-3. The telescope, gimbal, integrating sphere, and blackbody have components of constant weight plus components that scale with the telescope assembly outer diameter cubed. The instrument bench weight also contains fixed components and variable components that scale with diameter squared (telescope assembly outer diameter). The electronics and drive systems (motors/encoders) are assumed to be of constant weight.

Instrument power requirements are shown in Figure 4-4. Power scaling is constant except for the gimbal drive power. This peak power scales with the inertia of the rotating assembly. This peak power is consumed only briefly, when the gimbal accelerates or decelerates, therefore, the average power ends up being a fairly weak function of telescope aperture. Note that these numbers do not include any peak power associated with internal calibration either.

Telemetry requirements for GECS can be readily determined from ERBE experience plus GECS coverage time and ground resolution requirements. ERBE experience indicates about 1 kbps is required for instrument housekeeping and engineering data (voltages, temperature, etc.). Telemetry requirements for pointing and sensor data are a function of the system bandwidth and number of detector elements. Composite telemetry requirements for single and three

telescope configurations are shown in Figures 4-5 and 4-6, respectively. These plots assume three detector elements per telescope, each sampled at 12 bit resolution. Pointing data (elevation and azimuth position) is sampled with 16 bit resolution at the same rate as the detector data.

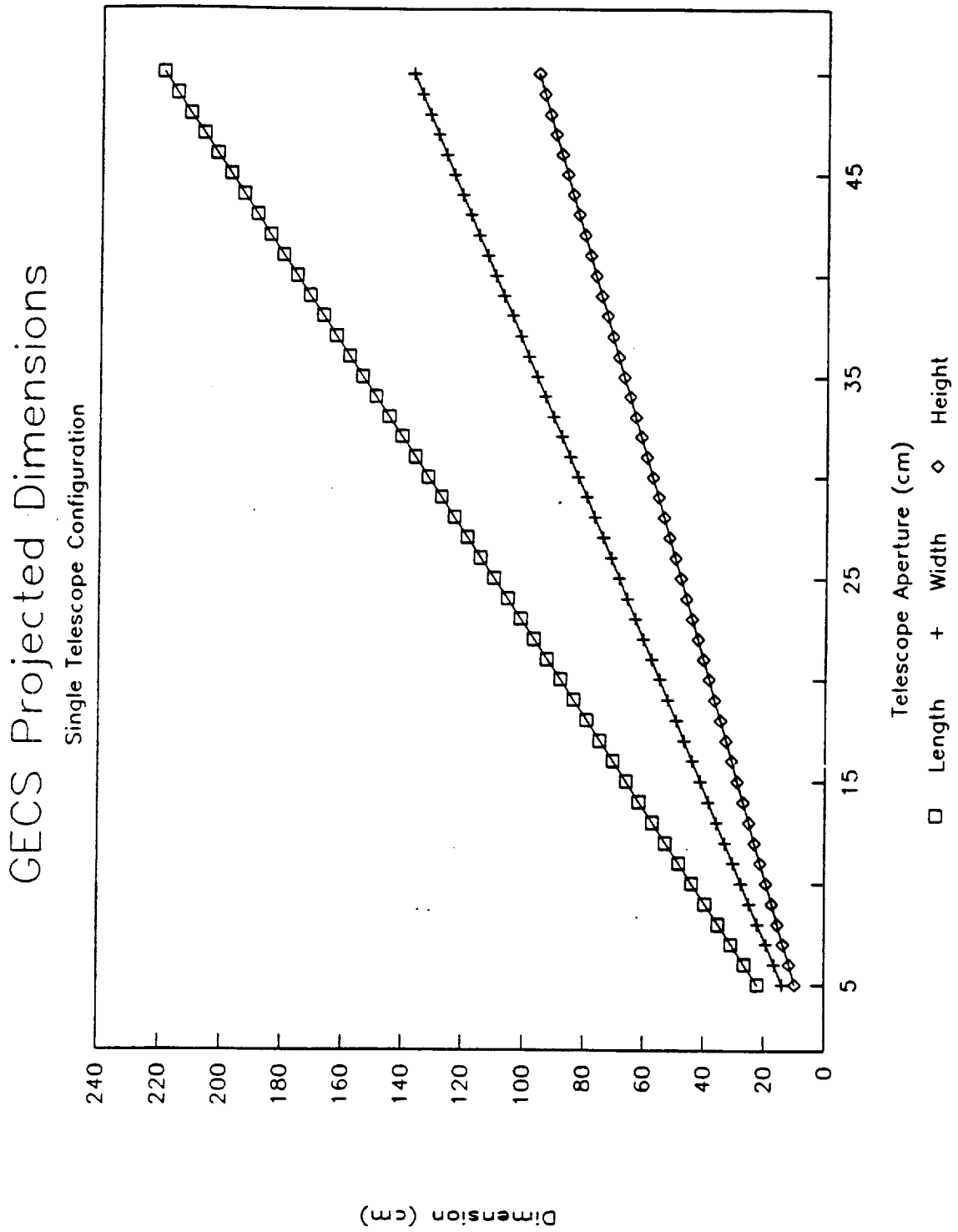


Figure 4-1

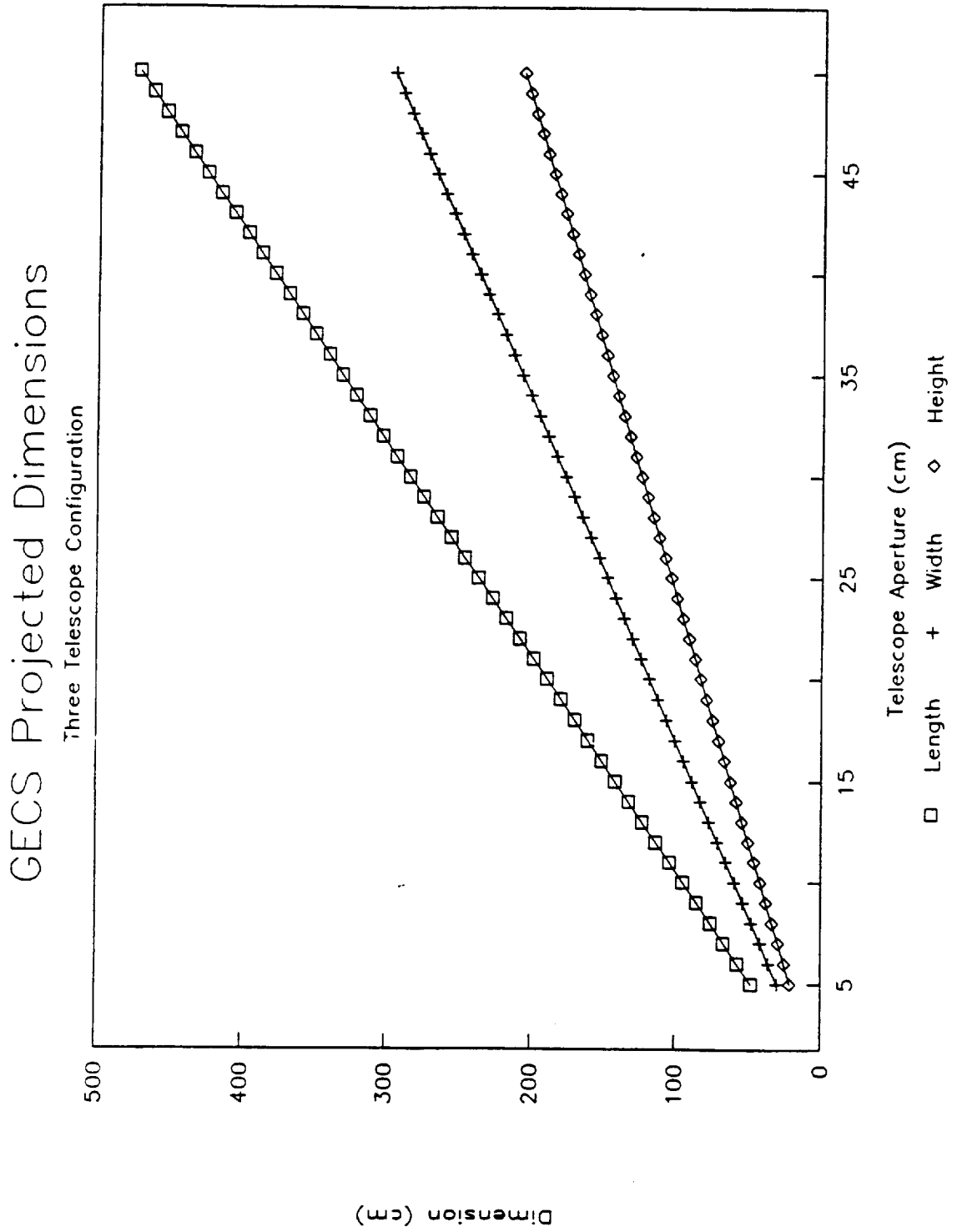


Figure 4-2

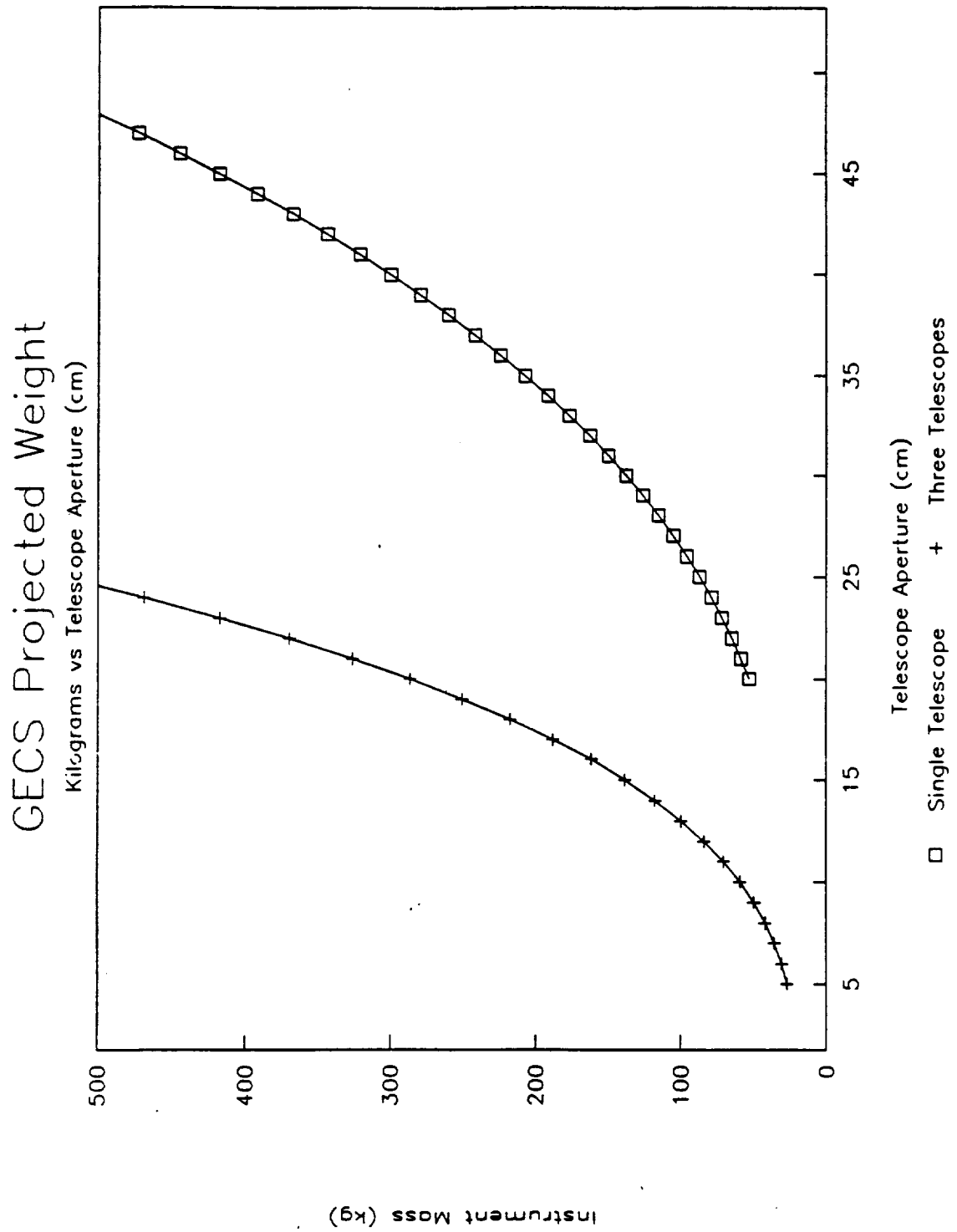


Figure 4-3

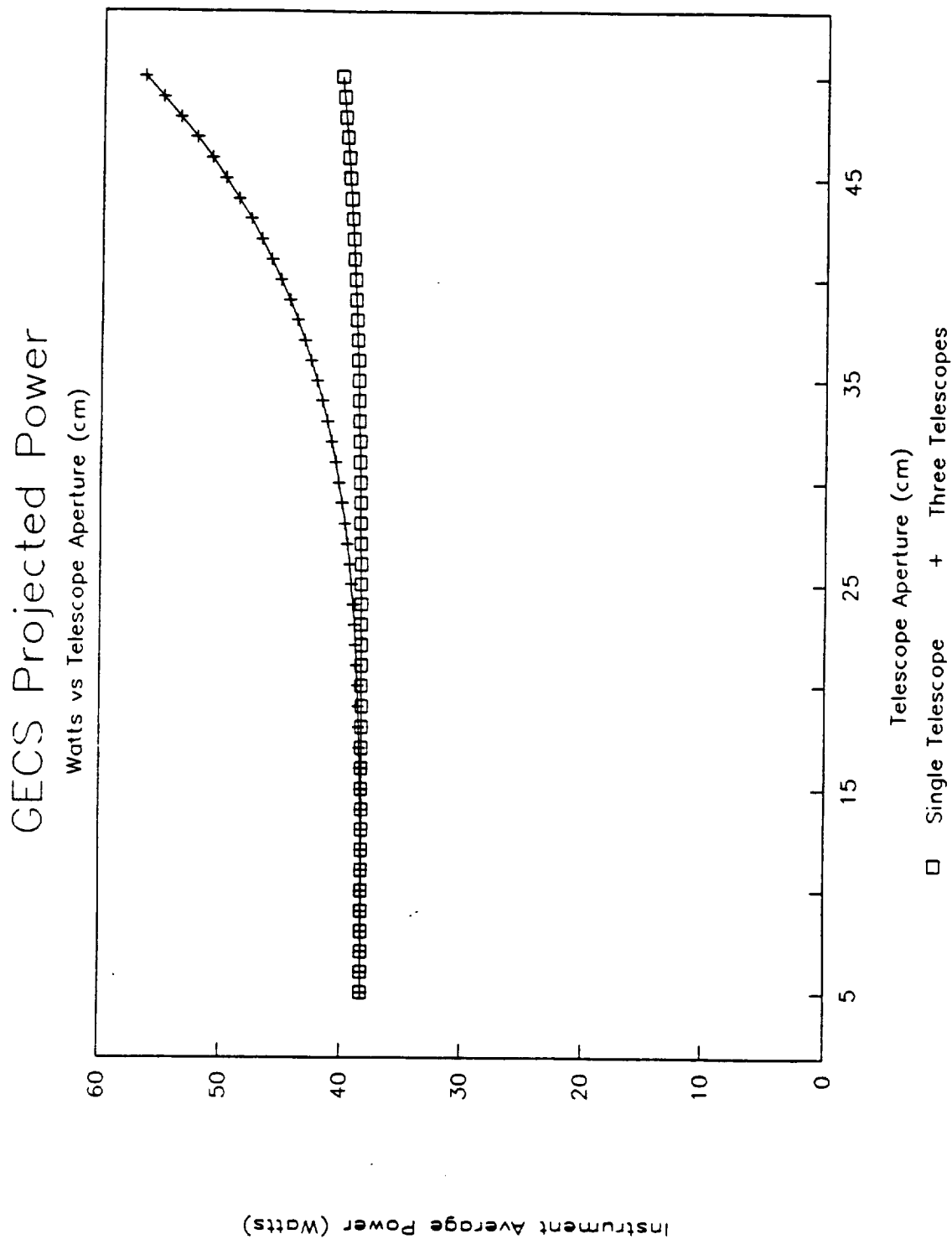


Figure 4-4

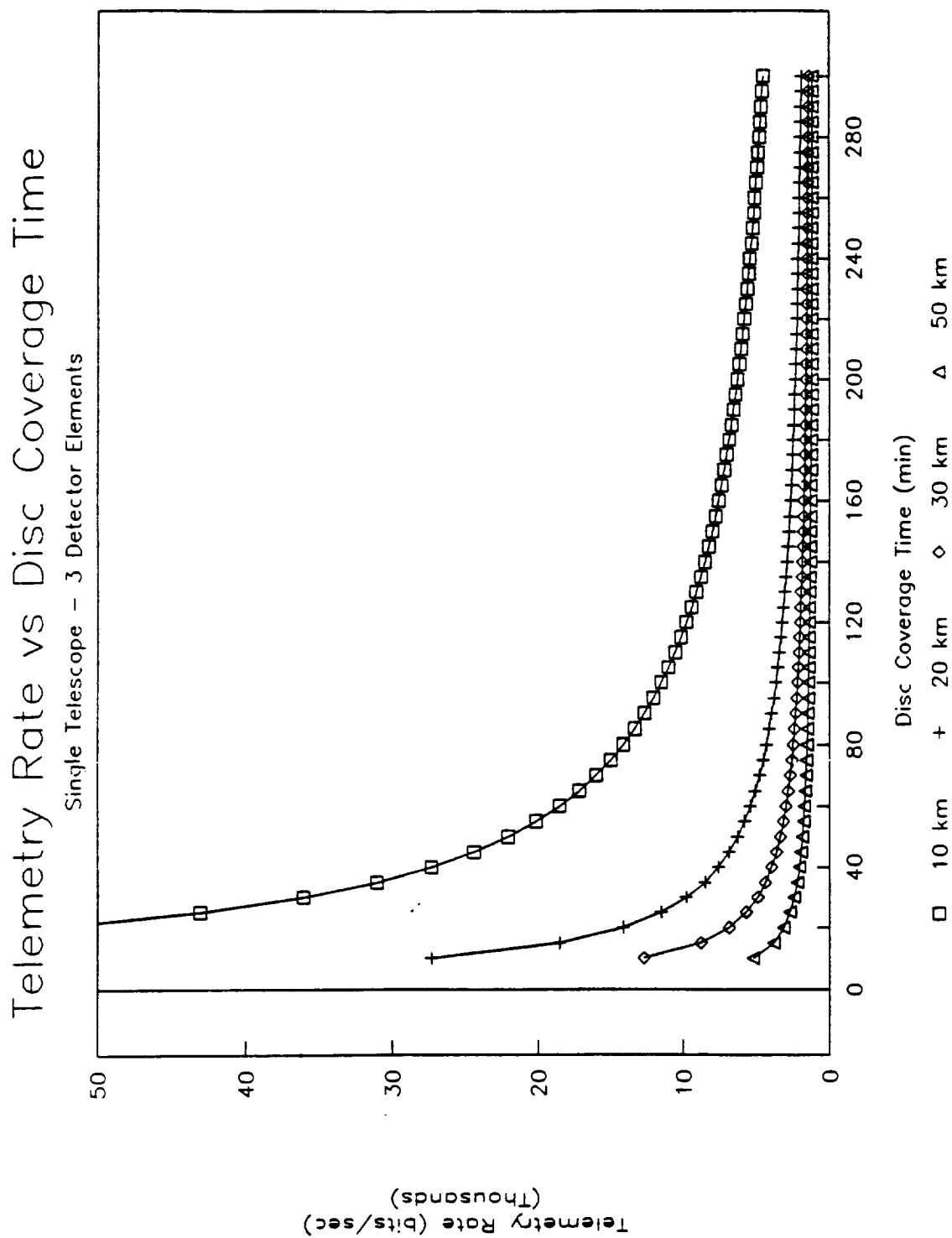


Figure 4-5

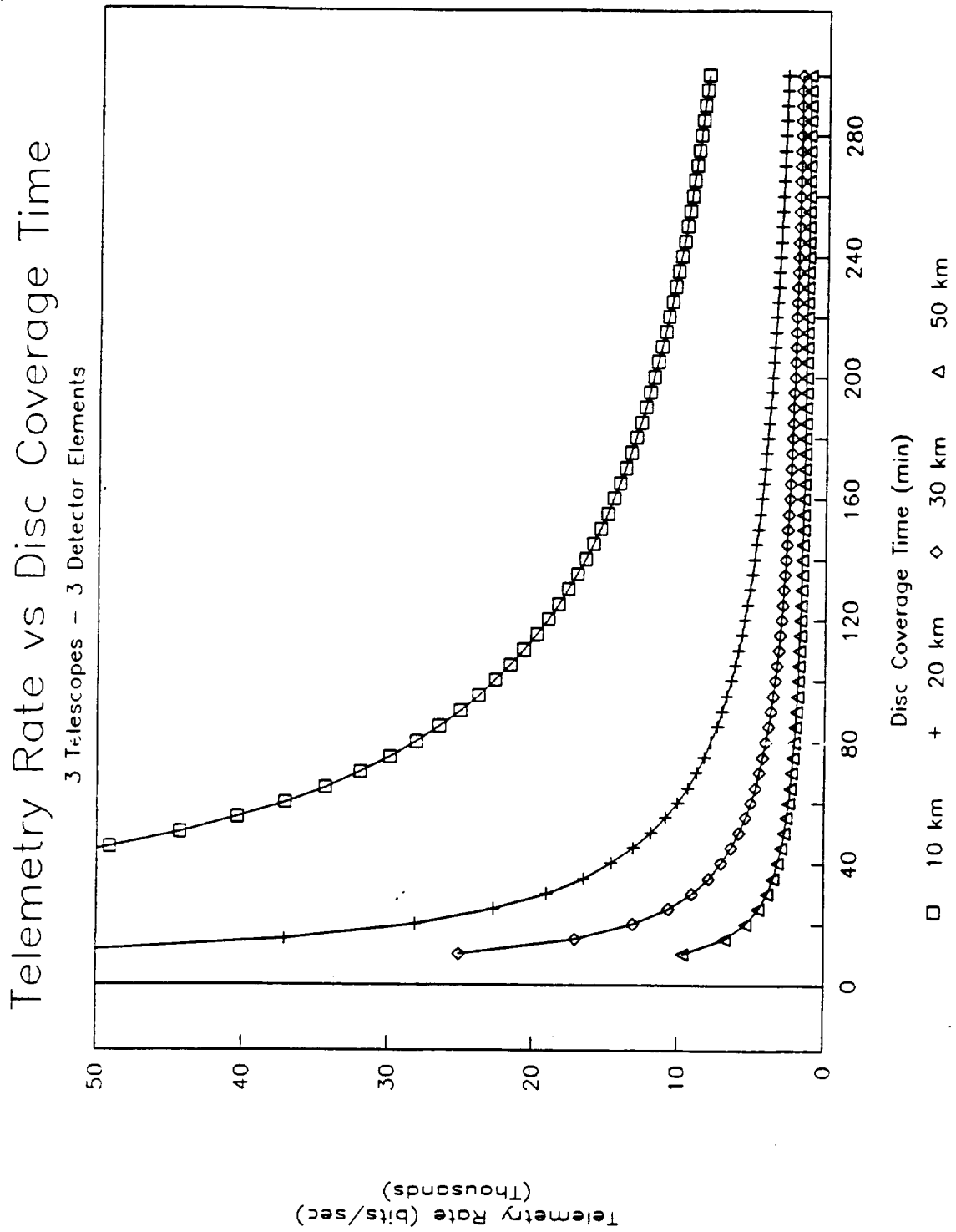


Figure 4-6

5.0 CALIBRATION

In-flight calibration of the GECS will follow the general approach used for ERBE and CERES. This approach employs full aperture longwave and shortwave calibration sources as components of the instrument design. Conceptually, the longwave in-flight calibration source is straight-forward and can employ a design similar to the ERBE Master Reference Blackbody (MRBB). This design uses a concentric grooved ring structure to provide high emissivity across all wavelengths of interest. Multiple Platinum Resistance Thermometers (PRT) embedded in the structure provide accurate data on the blackbody temperature and also monitor the spatial uniformity of the surface temperature. Patch heaters on the blackbody rear surface allow the source temperature to be varied which enables in-flight calibration of the instrument's dynamic response.

Implementation of the shortwave in-flight calibration source is less straight-forward, particularly as the aperture grows. The conceptual design employs an integrating sphere with output collimator similar to the concept currently being developed for CERES ground calibration. For GECS flight operation, the unit will provide options for solar and lamp illumination. The difficulty with this concept is scaling the design for large apertures. The integrating sphere efficiency suffers rapidly with increasing diameter, necessitating greatly increased input power to produce an output radiance of sufficient magnitude to be of value for in-flight calibration. This issue merits additional investigation during Phase B, with particular emphasis on adapting the Mirror Attenuator Mosaic (MAM) concept used for solar calibration on ERBE and on evaluating the evolving CERES integrating sphere design.

6.0 PHASE B RECOMMENDATIONS

Several issues have been identified during this Phase A study that warrant more in-depth consideration. Of particular interest are the following issues:

- 1) Regional vs. global coverage requirements
- 2) Detector development
- 3) Filter wheel options
- 4) Shortwave in-flight calibration

As discussed under system trades, the telescope aperture is driven by ground resolution and blur considerations. However, the detector size and telescope focal ratio are established by the system bandwidth, which is derived from global coverage time requirements. If the primary application of the instrument is regional studies, then these global coverage time requirements may prove to be inappropriate. If coverage requirements can be lowered, system bandwidth can be reduced and larger detector elements can be employed. This in turn will allow use of higher focal ratios in the telescope design, which could lead to simplifying the design back to the two element approach used for ERBE and CERES. The overall spectral response of the instrument would benefit from this trade.

Phase B study effort should also pursue detector development. Although the element sizes discussed for GECS have been produced routinely as immersed bolometer, the GECS elements must be non-immersed and require special coating/paint to enhance the responsivity over the broad spectral region. This responsivity enhancement is accomplished for CERES by cutting and bonding a thin paint flake with the necessary spectral response capabilities to the bolometer flake. These flakes are approximately 1.5 mm square, considerably larger than those envisioned for GECS. It is recommended that this issue be investigated with potential bolometer suppliers (SERVO) during Phase B.

Another area that merits additional thought is the use of various different waveband options in any design (such as the single telescope design) that employs a filter wheel for waveband selection. Such a design could include window channel as well as broadband longwave channel options. Since a typical filter wheel assembly can readily accommodate eight (sometimes more) openings, this would provide at least five "utility" channels for various special purposes.

A final topic that clearly needs greater attention is the issue of shortwave in-flight calibration. As discussed at the end of Section 5, the proposed approach has potential problems as the instrument aperture grows, and needs to be evaluated in greater detail to determine input power requirements necessary to produce sufficient output under these circumstances. These issues are being addressed by the CERES ground calibration effort, which may provide solutions adaptable to the GECS instrument. Phase B activity should also examine other shortwave in-flight calibration techniques such as solar diffusers and/or attenuators. Most notable of these techniques for study here is the Mirror Attenuator Mosaic (MAM) used for in-flight solar calibration on ERBE.

Appendix A

Design and analysis of the GECS optics was performed with the CODEV optical design code, a product of Optical Research Associates. A CODEV listing of the 16 cm aperture design is shown in an accompanying figure. The following is a short discussion of this listing.

The first line of the listing is a user specified title for the design. The title of this design was chosen to be *GECS F/1 OPTICS — 16 CM APERTURE*. The title is followed by a line of headings, of which the following are of interest here: RDY (radius of curvature), THI (thickness, or distance to next surface), RMD (specifies whether the surface is reflective), GLA (type of material for the surface). The remaining headings relate to constraints and variables used in the design process.

After the headings come a surface by surface description of the optical design. The first surface, OBJ, is the object, which is located at infinity and has an infinite radius of curvature (that is, the object is flat). The second surface is the primary mirror, labeled here by STO, since it is the stop for this design. Its radius of curvature is -51.37316 cm, and the distance from its center to the next surface is -17.044447 cm. The minus signs indicate the direction of curvature (convex or concave) and whether light is propagating forward or backward after reflection. The next three lines specify the conic constant of the mirror ($K=-1$ is a parabola), the curvature of the back side of the mirror (CUM), the thickness of the mirror (THM), and the material the mirror is made of (GLM). All the mirrors in this design were specified as fused silica. The next surface, labeled 2, is the secondary mirror. Its radius of curvature is -26.94295 cm, and the distance to the next surface is 25.1111 cm. It and all the remaining mirrors are spherical. Its back side is flat and its center

thickness is .688889 *cm*. The surface labeled 3 is a dummy surface located at the intermediate focus between the two pairs of mirrors. It is a flat surface (RDY=INFINITY), and the distance to the next surface (the third mirror) is 9.111111 *cm*. The surface labeled 4 is the tertiary mirror. Its radius of curvature is 3.12201 *cm*, it is 0.488889 *cm* thick with a flat back surface, and the distance to the next surface is -5.555556 *cm*. The surface labeled 5 is the quaternary mirror. Its radius of curvature is 8.64173 *cm*, it is 1.244444 *cm* thick with a curved back surface, and the distance to the next surface is 5.555556 *cm*. The surface labeled 6 is a flat dummy surface used in the design process. The distance from this surface to the image (IMG) is 5.978961 *cm*.

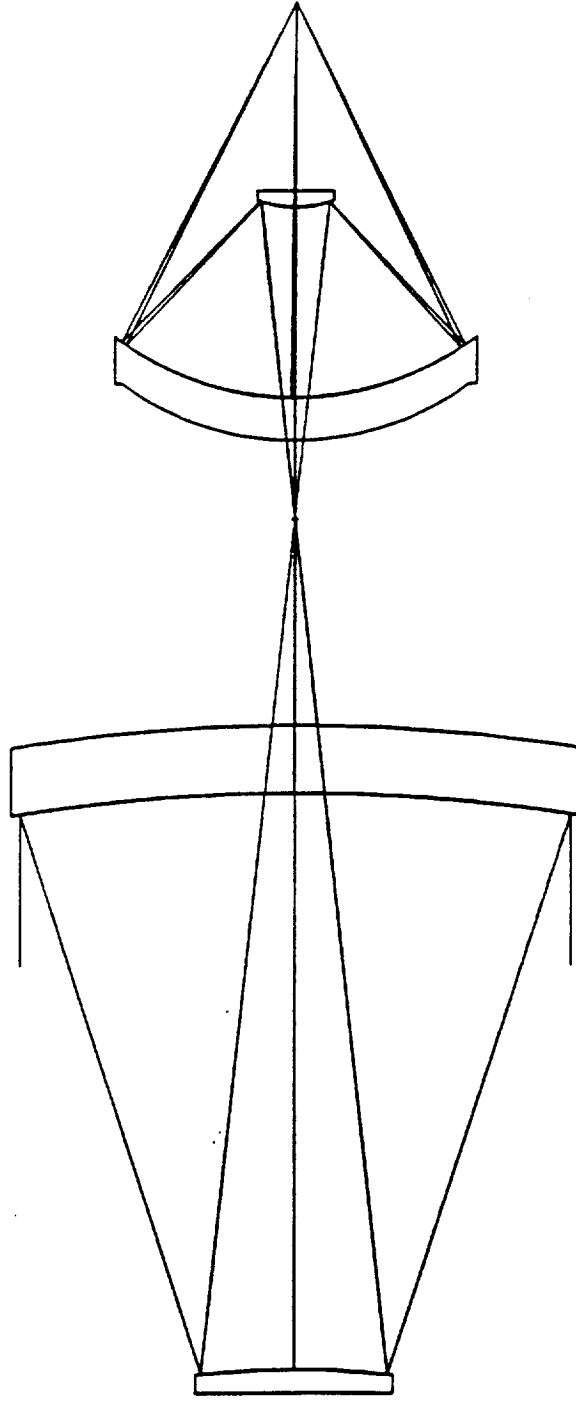
After the listing of the design comes a list of specification data. These include the entrance pupil diameter (EPD), dimensions for the design (centimeters), wavelength (not used here since this is an all reflective design), and field of view angles for points on the object (0.016 *degrees*).

Data under the next three headings is either not used or not important here.

Information under the last heading, infinite conjugates, lists paraxial information for an object at infinity. This data includes the effective focal length (EFL), back focal length measured from the last dummy surface (BFL), front focal length (FFL, not useful here), f number (FNO), image distance from last surface (IMG DIS), overall length from primary to tertiary of this design (OAL), and size and locations of the paraxial image and pupils.

10 : 50 : 37

PETERSON



GECS F/1 OPTICS --- 16 CM APERTURE

GLP 25-OCT-90

CODE V> LIST

GECS F/1 OPTICS --- 16 CM APERTURE

	RDY	THI	RMD	GLA	CCY	THC	GLC
> OBJ:	INFINITY	INFINITY			100	100	
STO:	-51.37316	-17.044447	REFL		0	1	
CON:							
K :	-1.000000	KC :	100				
CUM:	-0.019465	THM:	2.000000	GLM: SILICA_SPECIAL			
2:	-26.94295	25.111100	REFL		0	-1	
CUM:	0.000000	THM:	0.688889	GLM: SILICA_SPECIAL			
3:	INFINITY	9.111111			100	100	
4:	3.12201	-5.555556	REFL		0	100	
CUM:	0.000000	THM:	0.488889	GLM: SILICA_SPECIAL			
5:	8.64173	5.555556	REFL		UMY	100	
CUM:	0.115718	THM:	1.244444	GLM: SILICA_SPECIAL			
6:	INFINITY	5.978961			100	100	
IMG:	INFINITY	0.000000			100	100	

SPECIFICATION DATA

EPD	16.00000		
DIM	CM		
WL	50000.00		
REF	1		
WTW	1		
XAN	0.00000	0.00000	0.01600
YAN	0.00000	0.01600	0.01600
VUX	0.00000	0.00000	0.00000
VLX	0.00000	0.00000	0.00000
VUY	0.00000	0.00000	0.00000
VLY	0.00000	0.00000	0.00000

APERTURE DATA/EDGE DEFINITIONS

CA		
CIR S1	HOL	1.000000
CIR S4	HOL	0.444444

REFRACTIVE INDICES

GLASS CODE 50000.00
 INDEX data not specified for surface Obj thru 7

SOLVES

CUY S5 UMY 0.500000

This is a decentered system. If elements with power are decentered or tilted, the first order properties are probably inadequate in describing the system characteristics.

INFINITE CONJUGATES

EFL	-16.0000
BFL	5.9821
FFL	-637.5001
FNO	-1.0000
IMG DIS	5.9790
OAL	17.1778

PARAXIAL IMAGE

HT 0.0045
ANG 0.0160

ENTRANCE PUPIL

DIA 16.0000
THI 0.0000

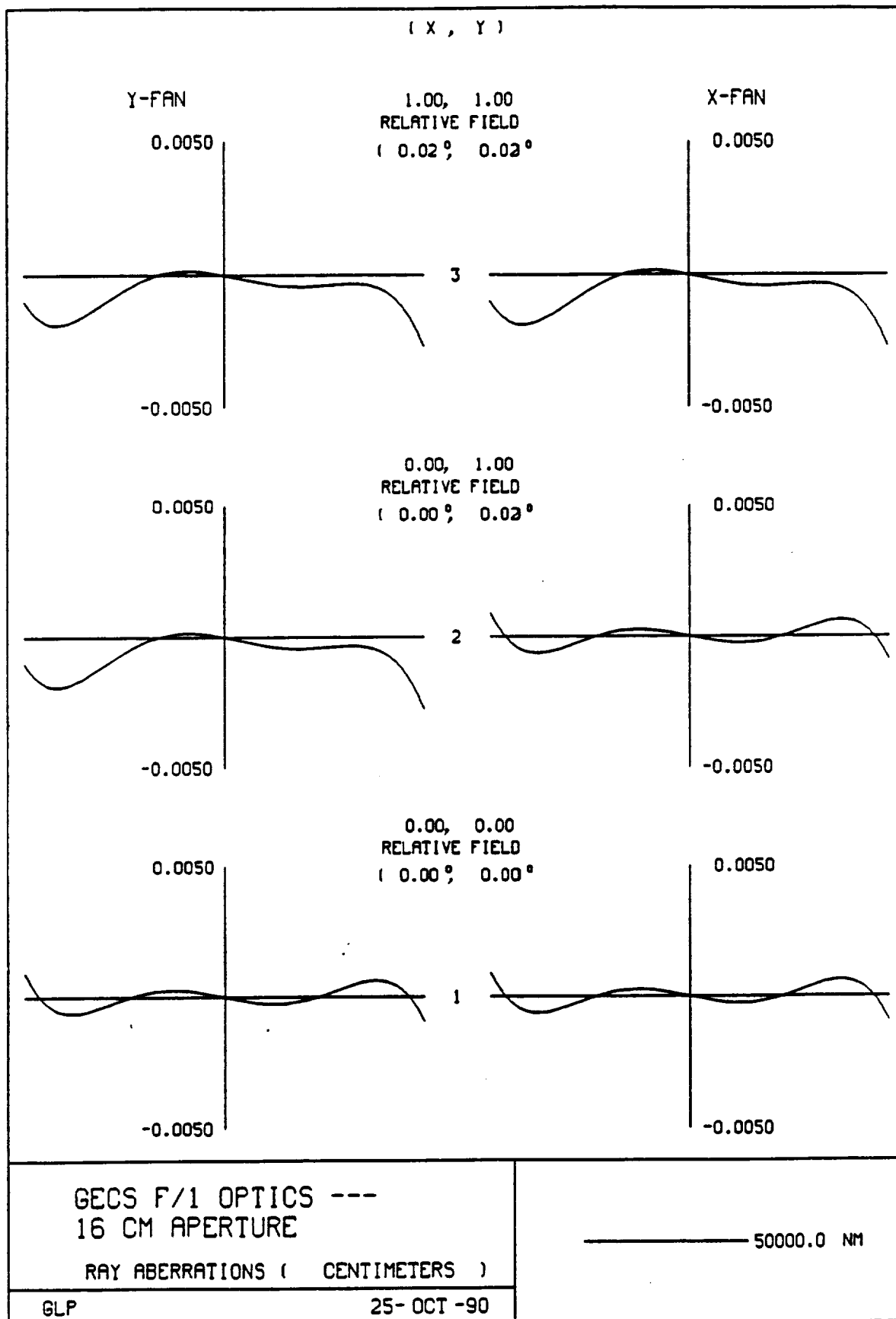
EXIT PUPIL

DIA 0.4016
THI 5.5806

CODE V> OUT T

PETERSON

10:47:59



FIELD
POSITION

1.00, 1.00
.0160, .0160 DG

0.00, 1.00
0.000, .0160 DG

0.00, 0.00
0.000, 0.000 DG

0.01000 CM

DEFOCUSING

0.00000

GECS F/1 OPTICS --- 16 CM APERTURE

PETERSON

10:49:0

The weights have been increased; too few points would have been plotted.
The new weights are 99

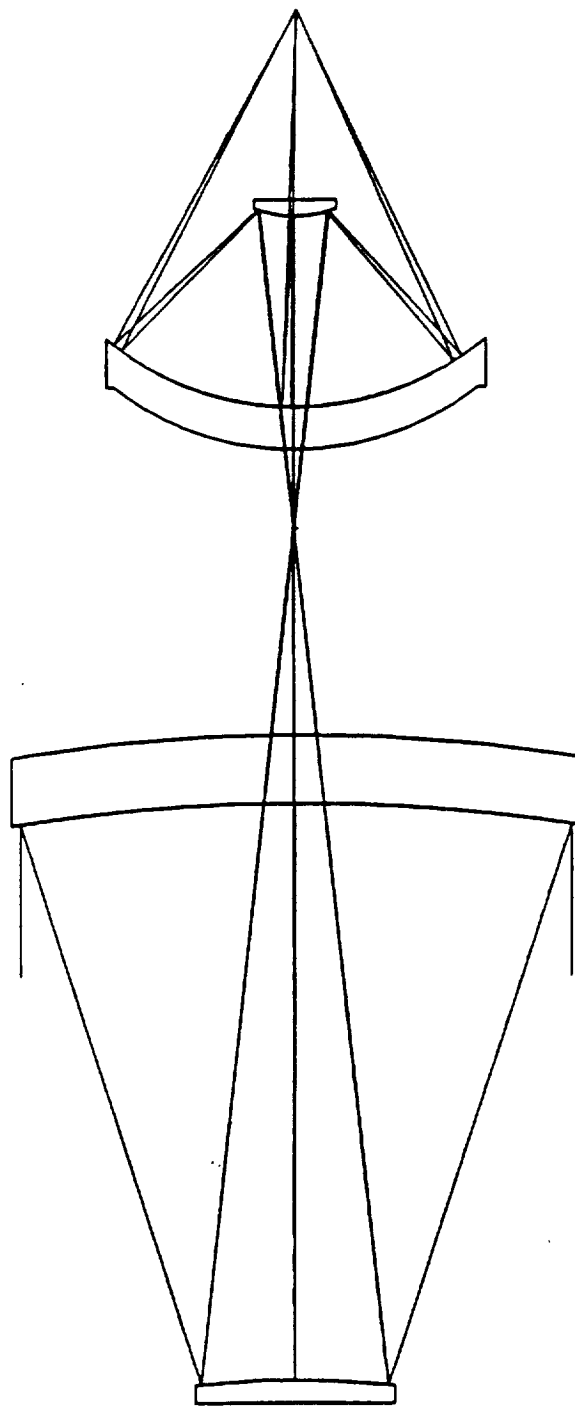
WAVELENGTH	WEIGHT	POINTS TRACED	POINTS ATTEMPTED	
50000.0	99	316	358	
Field 1, (0.00, 0.00) degrees. Focus 0.00000				
Displacement of centroid from chief ray				RMS spot diameter
X: 0.00000E+00	Y: 0.00000E+00			0.84036E-03 CM
Field 2, (0.00, 0.02) degrees. Focus 0.00000				
Displacement of centroid from chief ray				RMS spot diameter
X: 0.00000E+00	Y: -0.64641E-03			0.13532E-02 CM
Field 3, (0.02, 0.02) degrees. Focus 0.00000				
Displacement of centroid from chief ray				RMS spot diameter
X: -0.64240E-03	Y: -0.64240E-03			0.17200E-02 CM

Spot diagrams are not allowed to overlap. Points lying outside a
0.02461 X 0.02461 CM rectangle centered at the chief ray are not plotted.

RELATIVE FIELD HEIGHT	DEFOCUSING POSITION	TOTAL POINTS CALCULATED	POINTS NOT PLOTTED	PERCENTAGE OF POINTS PLOTTED
0.00, 0.00	1	316	0	100.0
0.00, 1.00	1	316	0	100.0
1.00, 1.00	1	314	0	100.0

11:4 :50

PETERSON



GECS F/1 OPTICS --- 16 CM APER./3 DET.

GLP 25-OCT -90

CODE V> LIST

GECS F/1 OPTICS --- 16 CM APER./3 DET.		GLA	CCY	THC	GLC
	RDY	THI	RMD		
> OBJ:	INFINITY	INFINITY		100	100
STO:	-51.37316	-17.044447	REFL	0	1
CON:					
K :	-1.000000	KC :	100		
CUM:	-0.019465	THM:	2.000000	GLM: SILICA_SPECIAL	
2:	-26.94295	25.111100	REFL	0	-1
CUM:	0.000000	THM:	0.688889	GLM: SILICA_SPECIAL	
3:	INFINITY	9.111111		100	100
4:	3.12201	-5.555556	REFL	0	100
CUM:	0.000000	THM:	0.488889	GLM: SILICA_SPECIAL	
5:	8.64173	5.555556	REFL	UMY	100
CUM:	0.115718	THM:	1.244444	GLM: SILICA_SPECIAL	
6:	INFINITY	5.978961		100	100
IMG:	INFINITY	0.000000		100	100

SPECIFICATION DATA

EPD	16.00000		
DIM		CM	
WL	50000.00		
REF	1		
WTW	1		
XAN	0.00000	0.00000	0.01600
YAN	0.01600	0.04800	0.04800
VUX	0.00000	0.00000	0.00000
VLX	0.00000	0.00000	0.00000
VUY	0.00000	0.00000	0.00000
VLY	0.00000	0.00000	0.00000

APERTURE DATA/EDGE DEFINITIONS

CA		
CIR S1	HOL	1.000000
CIR S4	HOL	0.444444

REFRACTIVE INDICES

GLASS CODE	50000.00
INDEX data not specified for surface Obj thru 7	

SOLVES

CUY S5	UMY	0.500000
--------	-----	----------

This is a decentered system. If elements with power are decentered or tilted, the first order properties are probably inadequate in describing the system characteristics.

INFINITE CONJUGATES

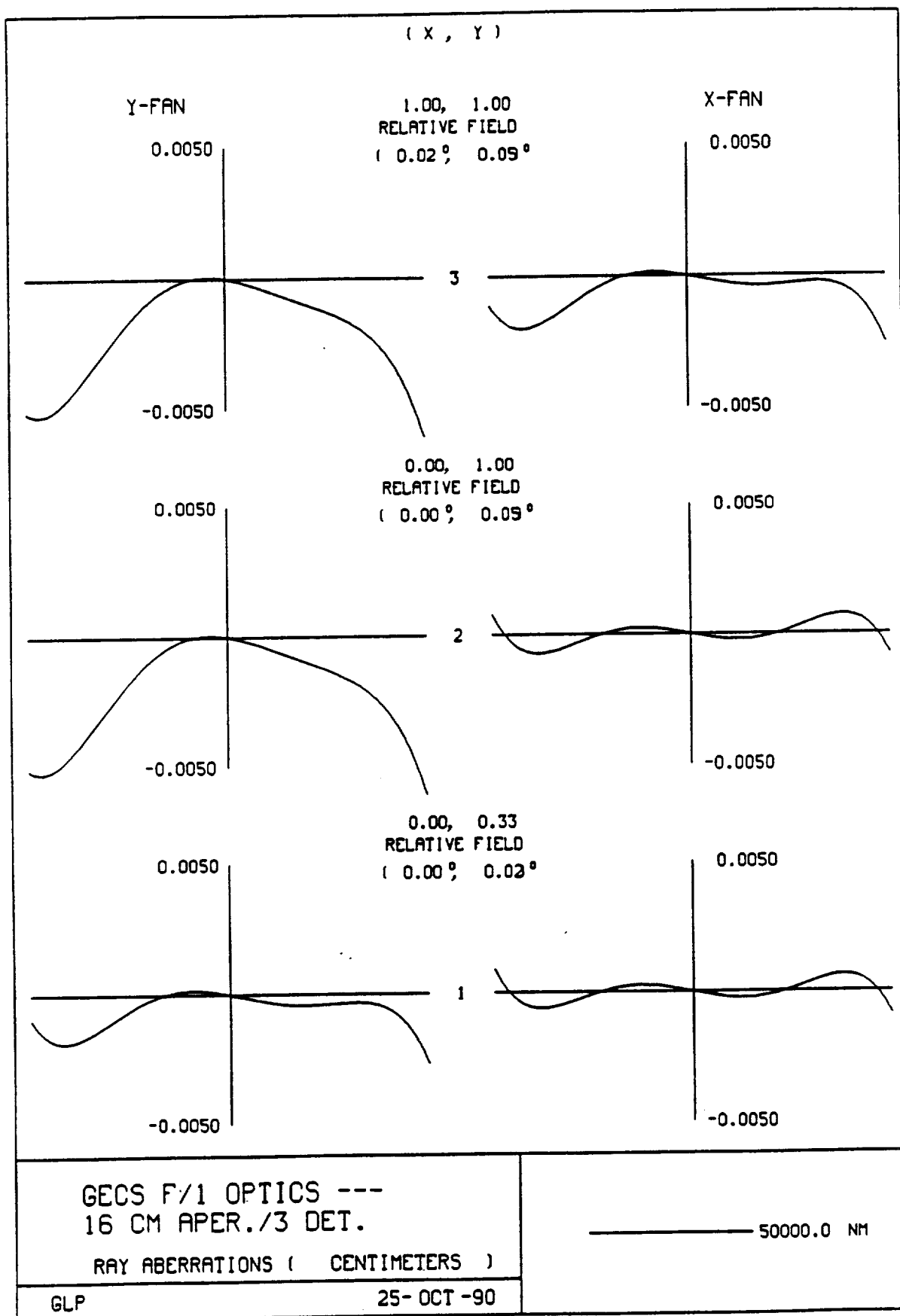
EFL	-16.0000
BFL	5.9821
FFL	-637.5001
FNO	-1.0000
IMG DIS	5.9790
OAL	17.1778
PARAXIAL IMAGE	

HT	0.0134
ANG	0.0480
ENTRANCE PUPIL	
DIA	16.0000
THI	0.0000
EXIT PUPIL	
DIA	0.4016
THI	5.5806

CODE V> OUT T

PETERSON

11:5 :37



FIELD
POSITION

1.00, 1.00
.0160, .0480 DG

0.00, 1.00
0.000, .0480 DG

0.00, 0.33
0.000, .0160 DG

0.01000 CM

DEFOCUSING

0.00000

GECS F/1 OPTICS --- 16 CM APER./3 DET.

PETERSON

11:6 :37

The weights have been increased; too few points would have been plotted.
The new weights are 99

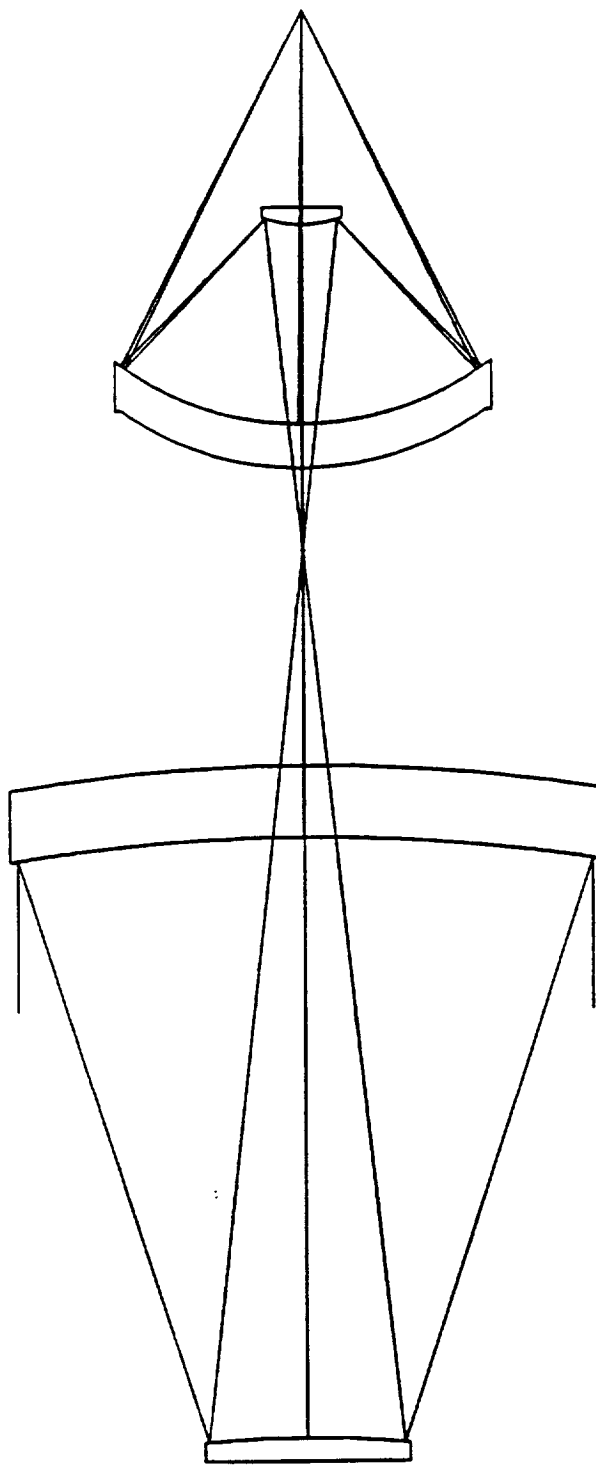
WAVELENGTH	WEIGHT	POINTS TRACED	POINTS ATTEMPTED	
50000.0	99	316	358	
Field 1, (0.00, 0.02) degrees. Focus 0.00000				
Displacement of centroid from chief ray				RMS spot diameter
X: 0.00000E+00	Y: -0.64639E-03			0.13531E-02 CM
Field 2, (0.00, 0.05) degrees. Focus 0.00000				
Displacement of centroid from chief ray				RMS spot diameter
X: 0.00000E+00	Y: -0.19417E-02			0.33179E-02 CM
Field 3, (0.02, 0.05) degrees. Focus 0.00000				
Displacement of centroid from chief ray				RMS spot diameter
X: -0.64732E-03	Y: -0.19420E-02			0.34897E-02 CM

Spot diagrams are not allowed to overlap. Points lying outside a
0.02461 X 0.02461 CM rectangle centered at the chief ray are not plotted.

RELATIVE FIELD HEIGHT	DEFOCUSING POSITION	TOTAL POINTS CALCULATED	POINTS NOT PLOTTED	PERCENTAGE OF POINTS PLOTTED
0.00, 0.33	1	316	0	100.0
0.00, 1.00	1	316	0	100.0
1.00, 1.00	1	316	0	100.0

11:25:2

PETERSON



7.50 CM

GECS F/1 OPTICS --- 25 CM APERTURE

GLP 25-OCT-90

CODE V> LIST

GECS F/1 OPTICS --- 25 CM APERTURE

	RDY	THI	RMD	GLA	CCY	THC	GLC
> OBJ:	INFINITY	INFINITY			100	100	
STO:	-80.27056	-26.631948	REFL		0	1	
CON:							
K :	-1.000000	KC :	100				
CUM:	-0.012458	THM:	3.125000	GLM: SILICA_SPECIAL			
2:	-42.09836		39.236094	REFL	0	-1	
CUM:	0.000000	THM:	1.076389	GLM: SILICA_SPECIAL			
3:	INFINITY		14.236111		100	100	
4:	4.87814		-8.680556	REFL	0	100	
CUM:	0.000000	THM:	0.763889	GLM: SILICA_SPECIAL			
5:	13.50271		8.680556	REFL	UMY	100	
CUM:	0.074059	THM:	1.944444	GLM: SILICA_SPECIAL			
6:	INFINITY		9.342127		100	100	
IMG:	INFINITY		0.000000		100	100	

SPECIFICATION DATA

EPD	25.00000		
DIM	CM		
WL	50000.00		
REF	1		
WTW	1		
XAN	0.00000	0.00000	0.01600
YAN	0.00000	0.01600	0.01600
VUX	0.00000	0.00000	0.00000
VLX	0.00000	0.00000	0.00000
VUY	0.00000	0.00000	0.00000
VLY	0.00000	0.00000	0.00000

APERTURE DATA/EDGE DEFINITIONS

CA		
CIR S1	HOL	1.562500
CIR S4	HOL	0.694444

REFRACTIVE INDICES

GLASS CODE 50000.00
 INDEX data not specified for surface Obj thru 7

SOLVES

CUY S5 UMY 0.500000

This is a decentered system. If elements with power are decentered or tilted, the first order properties are probably inadequate in describing the system characteristics.

INFINITE CONJUGATES

EFL	-25.0000
BFL	9.3471
FFL	-996.0939
FNO	-1.0000
IMG DIS	9.3421
OAL	26.8403

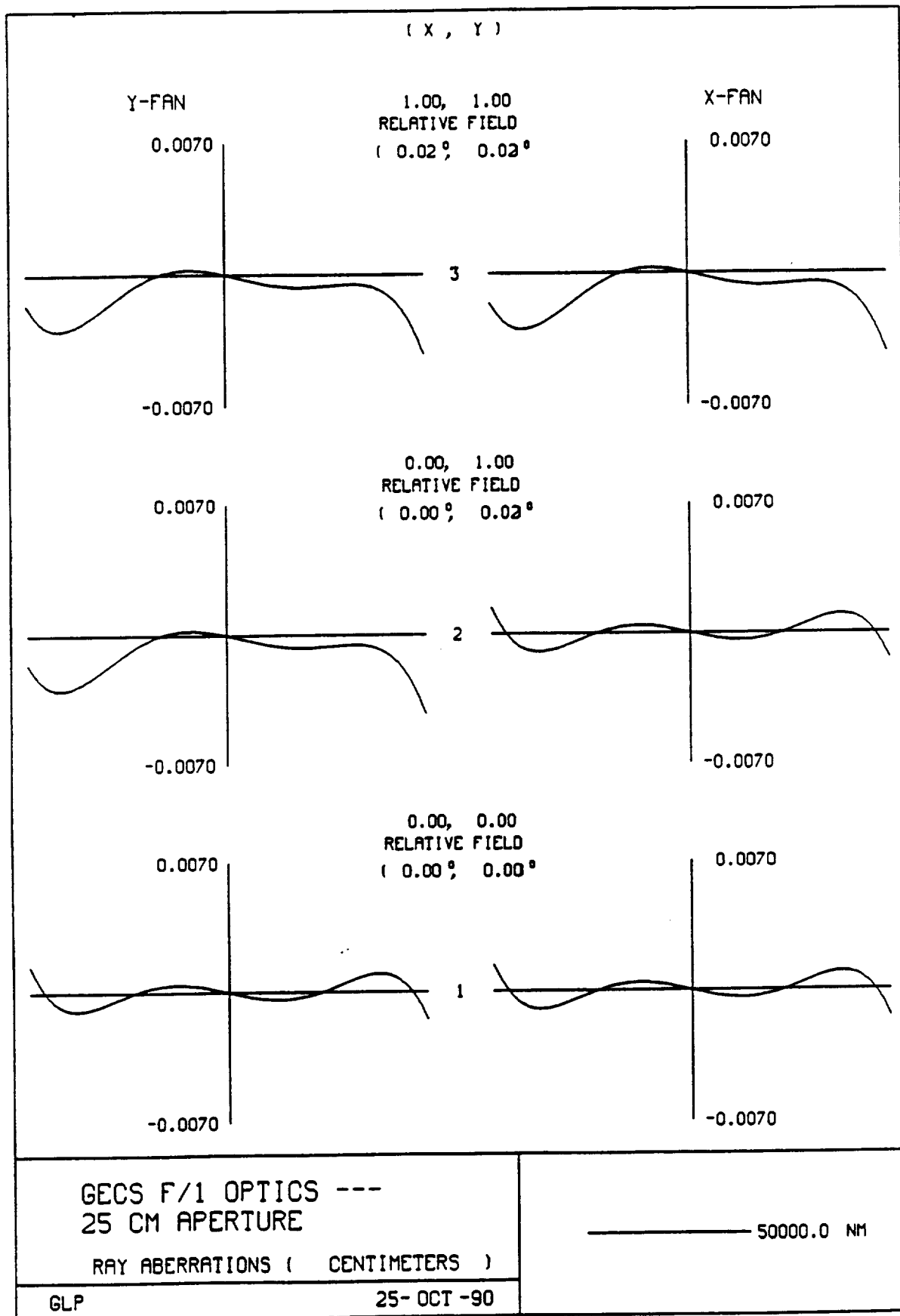
PARAXIAL IMAGE

HT	0.0070
ANG	0.0160
ENTRANCE PUPIL	
DIA	25.0000
THI	0.0000
EXIT PUPIL	
DIA	0.6275
THI	8.7196

CODE V> OUT T

PETERSON

11:22:32



FIELD
POSITION

1.00, 1.00
.0160, .0160 DG

0.00, 1.00
0.000, .0160 DG

0.00, 0.00
0.000, 0.000 DG

0.01400 CM

DEFOCUSING

0.00000

GECS F/1 OPTICS --- 25 CM APERTURE

PETERSON

11:23:40

The weights have been increased; too few points would have been plotted.
The new weights are 99

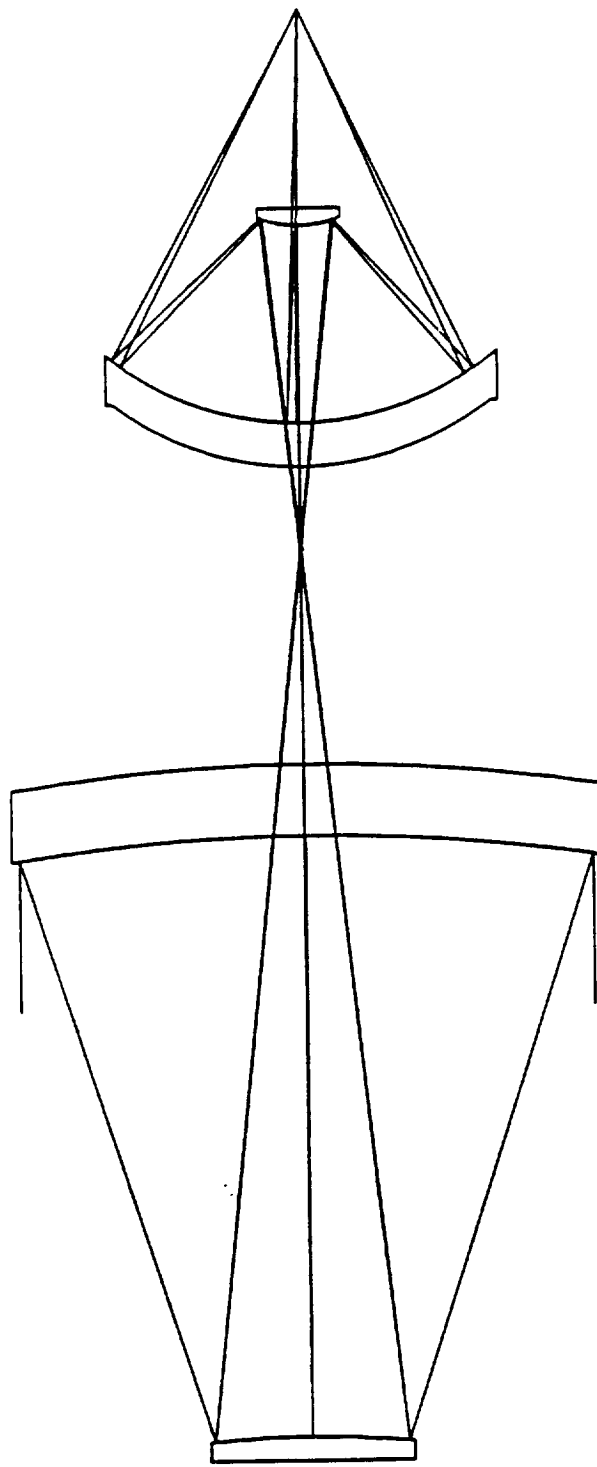
WAVELENGTH	WEIGHT	POINTS TRACED	POINTS ATTEMPTED	
50000.0	99	316	358	
Field 1, (0.00, 0.00) degrees. Focus 0.00000				
Displacement of centroid from chief ray				RMS spot diameter
X: 0.00000E+00	Y: 0.00000E+00			0.13131E-02 CM
Field 2, (0.00, 0.02) degrees. Focus 0.00000				
Displacement of centroid from chief ray				RMS spot diameter
X: 0.00000E+00	Y: -0.10100E-02			0.21143E-02 CM
Field 3, (0.02, 0.02) degrees. Focus 0.00000				
Displacement of centroid from chief ray				RMS spot diameter
X: -0.10038E-02	Y: -0.10038E-02			0.26874E-02 CM

Spot diagrams are not allowed to overlap. Points lying outside a
0.03445 X 0.03445 CM rectangle centered at the chief ray are not plotted.

RELATIVE FIELD HEIGHT	DEFOCUSING POSITION	TOTAL POINTS CALCULATED	POINTS NOT PLOTTED	PERCENTAGE OF POINTS PLOTTED
0.00, 0.00	1	316	0	100.0
0.00, 1.00	1	316	0	100.0
1.00, 1.00	1	314	0	100.0

12:38:8

PETERSON



GECS F/1 OPTICS --- 25 CM APER./3 DET.

GLP 25-OCT-90

CODE V> LIST

GECS F/1 OPTICS --- 25 CM APER./3 DET.		GLA	CCY	THC	GLC
	RDY	THI	RMD		
> OBJ:	INFINITY	INFINITY		100	100
STO:	-80.27056	-26.631948	REFL	0	1
CON:					
K :	-1.000000	KC :	100		
CUM:	-0.012458	THM:	3.125000	GLM: SILICA_SPECIAL	
2:	-42.09836	39.236094	REFL	0	-1
CUM:	0.000000	THM:	1.076389	GLM: SILICA_SPECIAL	
3:	INFINITY	14.236111		100	100
4:	4.87814	-8.680556	REFL	0	100
CUM:	0.000000	THM:	0.763889	GLM: SILICA_SPECIAL	
5:	13.50271	8.680556	REFL	UMY	100
CUM:	0.074059	THM:	1.944444	GLM: SILICA_SPECIAL	
6:	INFINITY	9.342127		100	100
IMG:	INFINITY	0.000000		100	100

SPECIFICATION DATA

EPD	25.00000		
DIM	CM		
WL	50000.00		
REF	1		
WTW	1		
XAN	0.00000	0.00000	0.01600
YAN	0.01600	0.04800	0.04800
VUX	0.00000	0.00000	0.00000
VLX	0.00000	0.00000	0.00000
VUY	0.00000	0.00000	0.00000
VLY	0.00000	0.00000	0.00000

APERTURE DATA/EDGE DEFINITIONS

CA	
CIR S1	HOL 1.562500
CIR S4	HOL 0.694444

REFRACTIVE INDICES

GLASS CODE 50000.00
 INDEX data not specified for surface Obj thru 7

SOLVES

CUY S5 UMY 0.500000

This is a decentered system. If elements with power are decentered or tilted, the first order properties are probably inadequate in describing the system characteristics.

INFINITE CONJUGATES

EFL	-25.0000
BFL	9.3471
FPL	-996.0939
FNO	-1.0000
IMG DIS	9.3421
OAL	26.8403

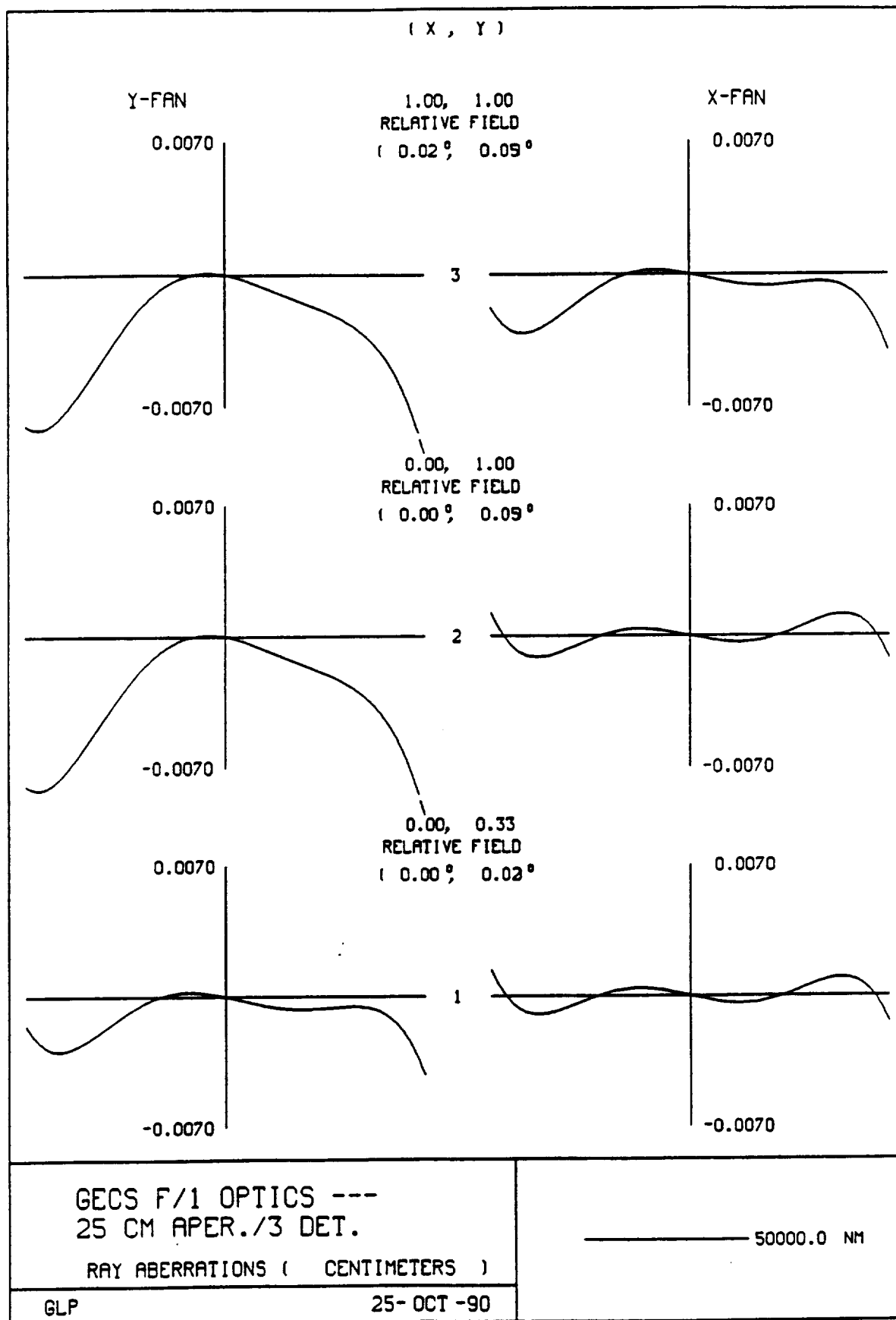
PARAXIAL IMAGE

HT	0.0209
ANG	0.0480
ENTRANCE PUPIL	
DIA	25.0000
THI	0.0000
EXIT PUPIL	
DIA	0.6275
THI	8.7196

CODE V> OUT T

PETERSON

12:38:52

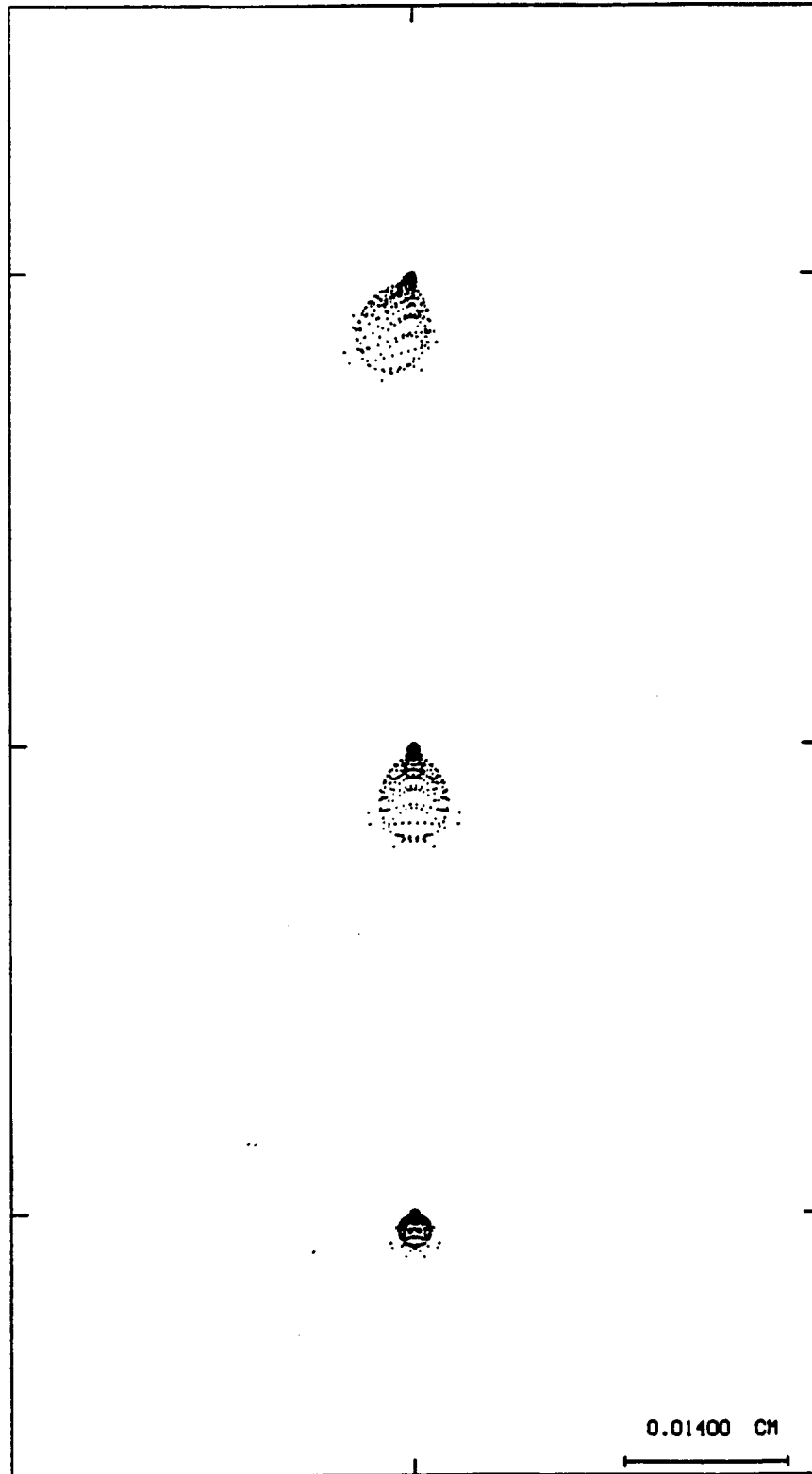


FIELD
POSITION

1.00, 1.00
.0160, .0480 DG

0.00, 1.00
0.000, .0480 DG

0.00, 0.33
0.000, .0160 DG



0.01400 CM

DEFOCUSING

0.00000

GECS F/1 OPTICS --- 25 CM APER./3 DET.

PETERSON

12:41:20

The weights have been increased; too few points would have been plotted.
The new weights are 99

WAVELENGTH	WEIGHT	POINTS TRACED	POINTS ATTEMPTED
50000.0	99	316	358

Field 1, (0.00, 0.02) degrees. Focus 0.00000	
Displacement of centroid from chief ray	RMS spot diameter
X: 0.00000E+00 Y: -0.10100E-02	0.21142E-02 CM

Field 2, (0.00, 0.05) degrees. Focus 0.00000	
Displacement of centroid from chief ray	RMS spot diameter
X: 0.00000E+00 Y: -0.30339E-02	0.51843E-02 CM

Field 3, (0.02, 0.05) degrees. Focus 0.00000	
Displacement of centroid from chief ray	RMS spot diameter
X: -0.10114E-02 Y: -0.30343E-02	0.54527E-02 CM

Spot diagrams are not allowed to overlap. Points lying outside a
0.03445 X 0.03445 CM rectangle centered at the chief ray are not plotted.

RELATIVE FIELD HEIGHT	DEFOCUSING POSITION	TOTAL POINTS CALCULATED	POINTS NOT PLOTTED	PERCENTAGE OF POINTS PLOTTE
0.00, 0.33	1	316	0	100.0
0.00, 1.00	1	316	0	100.0
1.00, 1.00	1	316	0	100.0